

Molecular structure of the $B_{s0}^*(5725)$ and $B_{s1}(5778)$ bottom-strange mesons

Amand Faessler, Thomas Gutsche, Valery E. Lyubovitskij ^{*}, Yong-Liang Ma

*Institut für Theoretische Physik, Universität Tübingen,
Auf der Morgenstelle 14, D-72076 Tübingen, Germany*

(Dated: June 11, 2008)

We discuss a possible interpretation of the scalar $B_{s0}^*(5725)$ and axial $B_{s1}(5778)$ bottom-strange mesons as hadronic molecules — bound states of BK and B^*K mesons, respectively. Using a phenomenological Lagrangian approach we analyze the strong $B_{s0}^* \rightarrow B_s\pi^0$, $B_{s1} \rightarrow B_s^*\pi^0$ and the radiative $B_{s0}^* \rightarrow B_s^*\gamma$, $B_{s1} \rightarrow B_s\gamma$, $B_{s1} \rightarrow B_s^*\gamma$, $B_{s1} \rightarrow B_{s0}^*\gamma$ decays. We give predictions for the decay properties: effective couplings and decay widths.

PACS numbers: 13.25.Hw, 13.40.Hq, 14.40.Nd

Keywords: bottom, charm and strange mesons, hadronic molecule, strong and radiative decay, isospin violation

^{*} On leave of absence from the Department of Physics, Tomsk State University, 634050 Tomsk, Russia

I. INTRODUCTION

Newly observed hadrons, in particular in the heavy flavor sector, have raised strong interest in treating and interpreting these states as hadronic bound states or, as commonly named, hadronic molecules (for overview see e.g. Ref. [1]). One of the main reasons to treat these observed states as molecules is that their masses are close to the thresholds of corresponding hadronic pairs. Canonical examples are the scalar $D_{s0}^*(2317)$ and axial $D_{s1}(2460)$ mesons. As stressed in [2] the scalar $D_{s0}^*(2317)$ and axial $D_{s1}(2460)$ mesons could be candidates for a scalar DK and a axial D^*K molecule because of a relatively small binding energy of ~ 50 MeV.

In a series of papers [3]-[7] we developed the quantum field approach based on phenomenological Lagrangians for the treatment of hadrons as bound states of lighter hadrons — hadronic molecules. In particular, we considered the strong, radiative and leptonic decays of $D_{s0}^*(2317)$ and $D_{s1}(2460)$ mesons [3]-[5]. A new feature related to the DK and D^*K molecular structure of the D_{s0}^* and D_{s1} mesons was that the presence of $u(d)$ quarks in the $D^{(*)}$ and K mesons gives rise to direct strong isospin-violating transitions $D_{s0}^* \rightarrow D_s\pi^0$ and $D_{s1} \rightarrow D_s^*\pi^0$ in addition to the decay mechanism induced by $\eta - \pi^0$ mixing, as considered previously. We showed that the direct transition compares with and even dominates over the $\eta - \pi^0$ mixing transition in the isospin-violating decays of D_{s0}^* and D_{s1} mesons. The composite (molecular) structure of the D_{s0}^* and D_{s1} mesons was defined by the compositeness condition $Z = 0$ [8, 9, 10] (see also Refs. [11] and [3]-[7]). This condition implies that the renormalization constant of the hadron wave function is set equal to zero or that the hadron exists as a bound state of its constituents. The compositeness condition was originally applied to the study of the deuteron as a bound state of proton and neutron [8]. Then it was extensively used in low-energy hadron phenomenology as the master equation for the treatment of mesons and baryons as bound states of light and heavy constituent quarks (see e.g. Refs. [9, 10]). We found that our theoretical framework gives numerical results which are consistent with both the experimental data and previous theoretical approaches.

In this paper we extend our formalism [3]-[7] to the scalar $B_{s0}^*(5725)$ and axial $B_{s1}(5778)$ bottom-strange mesons which have been considered before theoretically [12]-[28] as the bottom partners of the charm mesons D_{s0}^* and D_{s1} . In Ref. [16] masses, strong and radiative decays of B_{s0}^* and B_{s1} states have been analyzed using heavy hadron chiral perturbation theory. In particular, the mass spectrum, strong and radiative decays widths have been calculated using quark models, QCD sum rules, effective field approaches based on chiral and heavy quark symmetry including coupled-channel unitarity.

We assume that the $B_{s0}^*(5725)$ and $B_{s1}(5778)$ are bound states of BK and B^*K mesons, respectively. We adopt that the isospin, spin and parity quantum numbers of the B_{s0}^* (\bar{B}_{s0}^*) and B_{s1} (\bar{B}_{s1}) are $I(J^P) = 0(0^+)$ and $I(J^P) = 0(1^+)$, while for their masses we take the values $m_{B_{s0}^*} = 5725$ MeV and $m_{B_{s1}} = 5778$ MeV (the central values predicted in Refs. [20, 21]). Note, that different approaches result in the following ranges for the B_{s0}^* and B_{s1} masses: $m_{B_{s0}^*} = 5627 - 5841$ MeV and $m_{B_{s1}} = 5660 - 5859$ MeV. Using a phenomenological Lagrangian approach we analyze the strong $B_{s0}^* \rightarrow B_s\pi^0$, $B_{s1} \rightarrow B_s^*\pi^0$ and the radiative $B_{s0}^* \rightarrow B_s^*\gamma$, $B_{s1} \rightarrow B_s\gamma$, $B_{s1} \rightarrow B_s^*\gamma$, $B_{s1} \rightarrow B_{s0}^*\gamma$ decays. We give predictions for the decay properties: effective couplings and decay widths.

In the present manuscript we proceed as follows. First, in Sec. II, we outline our framework. We discuss the effective mesonic Lagrangian for the treatment of the B_{s0}^* and B_{s1} mesons as BK and B^*K bound states, respectively. In Section III we consider the matrix elements describing the strong and radiative decays of the B_{s0}^* and B_{s1} mesons. We discuss our numerical results and perform a comparison with other theoretical approaches. In Section IV we present a short summary of our results.

II. THEORETICAL FRAMEWORK

A. Molecular structure of the $B_{s0}^*(5725)$ and $B_{s1}(5778)$ mesons

In this section we discuss the formalism for the study of the $B_{s0}^*(5725)$ and $B_{s1}(5778)$ mesons as hadronic molecules, represented by a BK and B^*K bound state, respectively. We adopt that their quantum numbers (isospin, spin and parity) are $I(J^P) = 0(0^+)$ for B_{s0}^* (\bar{B}_{s0}^*) and $I(J^P) = 0(1^+)$ for B_{s1} (\bar{B}_{s1}). For their masses we take the values $m_{B_{s0}^*} = 5725$ MeV and $m_{B_{s1}} = 5778$ MeV (the central values predicted in Refs. [20, 21]). Our framework is based on an effective interaction Lagrangian describing the couplings of the B_{s0}^* and B_{s1} mesons to their constituents:

$$\mathcal{L}_{B_{s0}^*} = g_{B_{s0}^*} \bar{B}_{s0}^*(x) \int dy \Phi_{B_{s0}^*}(y^2) B^T(x + \omega_{KB} y) \bar{K}(x - \omega_{BK} y) + \text{H.c.}, \quad (1a)$$

$$\mathcal{L}_{B_{s1}} = g_{B_{s1}} \bar{B}_{s1}^\mu(x) \int dy \Phi_{B_{s1}}(y^2) B_\mu^{*T}(x + \omega_{KB^*} y) \bar{K}(x - \omega_{B^*K} y) + \text{H.c.}, \quad (1b)$$

where the doublets of B , B_μ^* and \bar{K} mesons are defined as

$$B = \begin{pmatrix} B^+ \\ B^0 \end{pmatrix}, \quad B_\mu^* = \begin{pmatrix} B^{*+} \\ B^{*0} \end{pmatrix}_\mu, \quad \bar{K} = \begin{pmatrix} K^- \\ \bar{K}^0 \end{pmatrix}. \quad (2)$$

The summation over isospin indices is understood and the symbol T refers to the transpose of the doublets B and B^* . The molecular structure of the B_{s0}^* and B_{s1} states is (we do not consider isospin mixing): $|B_{s0}^*\rangle = |B^+K^-\rangle + |B^0\bar{K}^0\rangle$, $|B_{s1}\rangle = |B^{*+}K^-\rangle + |B^{*0}\bar{K}^0\rangle$. In Eq. (1) we introduced the kinematical parameters $w_{ij} = m_i/(m_i + m_j)$, where $m_{i,j} = m_B$, m_{B^*} and m_K are the masses of B , B^* and K mesons. The correlation functions Φ_M with $M = B_{s0}^*$ or B_{s1} characterize the finite size of the B_{s0}^* and B_{s1} mesons as BK and B^*K bound states and depend on the relative Jacobi coordinate y with, in addition, x being the center of mass (CM) coordinate. Note, that the local limit corresponds to the substitution of Φ_M by the Dirac delta-function: $\Phi_M(y^2) \rightarrow \delta^4(y)$. A basic requirement for the choice of an explicit form of the correlation function is that its Fourier transform vanishes sufficiently fast in the ultraviolet region of Euclidean space to render the Feynman diagrams ultraviolet finite. We adopt the Gaussian form, $\tilde{\Phi}_M(p_E^2/\Lambda_M^2) \doteq \exp(-p_E^2/\Lambda_M^2)$, for the Fourier transform of vertex function, where p_E is the Euclidean Jacobi momentum. Here $\Lambda_{B_{s0}^*}$ is a size parameter, which parametrizes the distribution of B and K mesons inside the B_{s0}^* molecule, while $\Lambda_{B_{s1}}$ is the size parameter for the B_{s1} molecule. For simplicity we will use a universal scale parameter $\Lambda_M = \Lambda_{B_{s0}^*} = \Lambda_{B_{s1}}$.

The coupling constants $g_{B_{s0}^*}$ and $g_{B_{s1}}$ are determined by the compositeness condition [8, 9], which implies that the renormalization constant of the hadron wave function is set equal to zero:

$$Z_{B_{s0}^*} = 1 - \Sigma'_{B_{s0}^*}(m_{B_{s0}^*}^2) = 0, \quad (3a)$$

$$Z_{B_{s1}} = 1 - \Sigma'_{B_{s1}}(m_{B_{s1}}^2) = 0. \quad (3b)$$

Here, $\Sigma'_{B_{s0}^*}(m_{B_{s0}^*}^2) = g_{B_{s0}^*}^2 \Pi'_{B_{s0}^*}(m_{B_{s0}^*}^2)$ is the derivative of the B_{s0}^* meson mass operator. In the case of the B_{s1} meson we have $\Sigma'_{B_{s1}}(m_{B_{s1}}^2) = g_{B_{s1}}^2 \Pi'_{B_{s1}}(m_{B_{s1}}^2)$, which is the derivative of the transverse part of its mass operator $\Sigma_{B_{s1}}^{\mu\nu}$, conventionally split into transverse $\Sigma_{B_{s1}}$ and longitudinal $\Sigma_{B_{s1}}^L$ parts as:

$$\Sigma_{B_{s1}}^{\mu\nu}(p) = g_{\perp}^{\mu\nu} \Sigma_{B_{s1}}(p^2) + \frac{p^\mu p^\nu}{p^2} \Sigma_{B_{s1}}^L(p^2), \quad (4)$$

where

$$g_{\perp}^{\mu\nu} = g^{\mu\nu} - \frac{p^\mu p^\nu}{p^2}, \quad g_{\perp}^{\mu\nu} p_\mu = 0. \quad (5)$$

The mass operators of the B_{s0}^* and B_{s1} mesons are described by the diagrams of Fig. 1(a) and 1(b), respectively.

Following Eqs. (3a) and (3b) the coupling constants $g_{B_{s0}^*}$ and $g_{B_{s1}}$ can be expressed in the form:

$$\frac{1}{g_{B_{s0}^*}^2} = \frac{2}{(4\pi\Lambda_M)^2} \int_0^1 dx \int_0^\infty d\alpha \alpha P_0(\alpha, x) \left[-\frac{d}{dz_0} \tilde{\Phi}_M^2(z_0) \right], \quad (6a)$$

$$\frac{1}{g_{B_{s1}}^2} = \frac{2}{(4\pi\Lambda_M)^2} \int_0^1 dx \int_0^\infty d\alpha \alpha P_1(\alpha, x) \left[\frac{1}{2\mu_{B^*}^2(1+\alpha)} - \frac{d}{dz_1} \right] \tilde{\Phi}_M^2(z_1) \quad (6b)$$

where

$$\begin{aligned} P_0(\alpha, x) &= \alpha^2 x(1-x) + w_{BK}^2 \alpha x + w_{KB}^2 \alpha(1-x), \\ P_1(\alpha, x) &= \alpha^2 x(1-x) + w_{B^*K}^2 \alpha x + w_{KB^*}^2 \alpha(1-x), \\ z_0 &= \mu_B^2 \alpha x + \mu_K^2 \alpha(1-x) - \frac{P_0(\alpha, x)}{1+\alpha} \mu_{B_{s0}^*}^2, \\ z_1 &= \mu_{B^*}^2 \alpha x + \mu_K^2 \alpha(1-x) - \frac{P_1(\alpha, x)}{1+\alpha} \mu_{B_{s1}}^2, \\ \mu_M &= \frac{m_M}{\Lambda_M}. \end{aligned} \quad (7)$$

The above expressions are valid for any functional form of the correlation function $\tilde{\Phi}_M$.

Note that the compositeness condition of the type (3a), (3b) was originally applied to the study of the deuteron as a bound state of proton and neutron [8]. Then this condition was extensively used in low-energy hadron phenomenology as the master equation for the treatment of mesons and baryons as bound states of light and heavy constituent quarks [9, 10]. In Refs. [11] and [3]-[7] this condition was used in the application to hadronic molecule configurations of light and heavy mesons.

B. Effective Lagrangian for strong and radiative decays of B_{s0}^* and B_{s1} mesons

In Ref. [3, 5], in the analysis of the strong isospin-violating decays $D_{s0}^* \rightarrow D_s\pi^0$ and $D_{s1} \rightarrow D_s^*\pi^0$ in the molecular approach, we showed the existence of two possible dynamical mechanisms. This included the so-called “direct” mechanism with π^0 -meson emission from the $D \rightarrow D^*$ and $K \rightarrow K^*$ transitions and the “indirect” mechanism where a π^0 meson is produced via $\eta - \pi^0$ mixing. The mixing is due to the mass term of pseudoscalar mesons in the leading-order $O(p^2)$ Lagrangian of chiral perturbation theory (ChPT) [29, 30]. Note, that the second mechanism based on $\eta - \pi^0$ mixing was mainly considered before in the literature. Originally it was initiated by the analysis based on the use of chiral Lagrangians [16, 30, 31, 32] where the leading-order, tree-level $D_{s0}^*D_s\pi^0$ ($D_{s1}D_s^*\pi^0$) coupling can be generated only by virtual η -meson emission. In Ref. [5] we showed that the “direct” and “mixing” mechanisms can be combined together in the form of an effective coupling of π^0 to the mesonic pairs DD^* or KK^* with modified flavor structure. This modification occurs after the diagonalization of the mesonic mass term involving π^0 and η meson fields [29] (see details in [5]). In particular, instead of the $\tau_3 \pi^0$ coupling to DD^* or KK^* we have $\pi^0 (\tau_3 \cos \varepsilon + \kappa I \sin \varepsilon)$, where $\kappa = 1/\sqrt{3}$ or $\sqrt{3}$ is the corresponding flavor-algebra factor for the DD^* or KK^* coupling, respectively. The $\pi^0 - \eta$ mixing angle ε is fixed as [29]:

$$\tan 2\varepsilon = \frac{\sqrt{3}}{2} \frac{m_d - m_u}{m_s - \hat{m}} \simeq 0.02, \quad \hat{m} = \frac{1}{2}(m_u + m_d), \quad (8)$$

where m_u, m_d, m_s are the current quark masses.

Below, in Eq.(11), we display the explicit form of the corresponding interaction Lagrangian. The lowest-order diagrams which contribute to the matrix elements of the strong isospin-violating decays $B_{s0}^* \rightarrow B_s\pi^0$ and $B_{s1} \rightarrow B_s^*\pi^0$ are shown in Figs.2 and 3. Note, that in the isospin limit ($m_u = m_d$), the $\eta - \pi^0$ mixing angle vanishes and the masses of the virtual $B^{(*)}$ and $K^{(*)}$ mesons in the loops are degenerate. As a result the pairs of diagrams related to Figs.2(a) and 2(b), Figs.2(c) and 2(d), Figs.3(a) and 3(b), Figs.3(c) and 3(d) compensate each other. Therefore, in the calculation of the diagrams of Figs.2 and 3 we go beyond the isospin limit and use the physical meson masses.

The diagrams contributing to the radiative decays $B_{s0}^* \rightarrow B_s^*\gamma$, $B_{s1} \rightarrow B_s\gamma$, $B_{s1} \rightarrow B_s^*\gamma$ and $B_{s1} \rightarrow B_{s0}^*\gamma$ are shown in Figs.4, 5, 6 and 7. The diagrams of Figs.4(a), 4(b), 5(a) and 5(b) are generated by the direct coupling of the charged K^- and $B^+(B^{*+})$ mesons to the electromagnetic field after gauging the free Lagrangians related to these mesons. The diagrams of Figs.6(a)-6(d), 7(a) and 7(b) are generated by the coupling of a corresponding pair of vector and pseudoscalar mesons to the photon. The diagrams of Figs.4(c), 5(c), and 6(e) are generated after gauging the nonlocal strong Lagrangians (1) describing the coupling of the B_{s0}^* and B_{s1} mesons to their constituents. The diagrams of Figs.4(d) and 5(d) arise after gauging the strong $B_s^*B^+K^-$ and $B_sB^{*+}K^-$ interaction Lagrangian containing derivatives acting on the pseudoscalar fields. Details of how to generate the effective couplings of the involved mesons to the electromagnetic field will be discussed later.

After the preliminary discussion of the relevant diagrams, we are now in the position to write down the full effective Lagrangian for the study of the strong and radiative decays of the B_{s0}^* and B_{s1} mesons formulated in terms of mesonic degrees of freedom and of photons. We follow the procedure discussed in detail in Refs. [3]-[5], where we considered the D_{s0}^* and D_{s1} meson decay properties. First, we write the Lagrangian \mathcal{L} , which includes the free mesonic parts $\mathcal{L}_{\text{free}}$ and the strong interaction parts \mathcal{L}_{str} :

$$\mathcal{L}(x) = \mathcal{L}_{\text{free}}(x) + \mathcal{L}_{\text{str}}(x), \quad (9)$$

with

$$\begin{aligned} \mathcal{L}_{\text{free}}(x) &= -\bar{B}_{s0}^{*+}(x)(\square + m_{B_{s0}^*}^2)B_{s0}^*(x) + \bar{B}_{s1,\mu}(x)(g^{\mu\nu}[\square + m_{B_{s1}}^2] - \partial^\mu\partial^\nu)B_{s1,\nu}(x) \\ &- \frac{1}{2}\vec{\pi}(x)(\square + m_\pi^2)\vec{\pi}(x) + \frac{\delta_\pi}{2}[\pi^0(x)]^2 - \sum_{P=K,B,B_s} P^\dagger(x)(\square + m_P^2)P(x) + \sum_{P=K,B} \delta_P \bar{P}^0(x)P^0(x) \\ &+ \sum_{V=K^*,B^*,B_s^*} V_\mu^\dagger(x)(g^{\mu\nu}[\square + m_V^2] - \partial^\mu\partial^\nu)V_\nu(x) - \sum_{V=K^*,B^*} \delta_V \bar{V}_\mu^0(x)V^{0\mu}(x), \end{aligned} \quad (10)$$

$$\begin{aligned}
\mathcal{L}_{\text{str}}(x) = & \frac{g_{B^*B\pi}}{2\sqrt{2}} B_\mu^{*\dagger}(x) \hat{\pi}_B(x) i \overleftrightarrow{\partial}^\mu B(x) + \frac{g_{K^*K\pi}}{\sqrt{2}} K_\mu^{*\dagger}(x) \hat{\pi}_K(x) i \overleftrightarrow{\partial}^\mu K(x) \\
& + g_{B_s B^* K} B_\mu^{*\dagger}(x) K(x) i \overleftrightarrow{\partial}^\mu B_s^0(x) + g_{B_s B K^*} K_\mu^{*\dagger}(x) B(x) i \overleftrightarrow{\partial}^\mu \bar{B}_s^0(x) + g_{B_s^* B K} B_{s,\mu}^{*0}(x) B^\dagger(x) i \overleftrightarrow{\partial}^\mu K(x) \\
& - ig_{B_s^* B^* K^*} \left[B_s^{*0\mu\nu}(x) B_\mu^{*\dagger}(x) K_\nu(x) + B_{\mu\nu}^{*\dagger}(x) K^{*\mu}(x) B_s^{*0\nu}(x) + K^{*\mu\nu}(x) B_{s,\mu}^{*0}(x) B_\nu^{*\dagger}(x) \right] \\
& + \frac{g_{B_s^* B^* K}}{4} \epsilon^{\mu\nu\alpha\beta} B_{s\mu\nu}^*(x) B_{\alpha\beta}^{*\dagger}(x) K(x) + \mathcal{L}_{B_{s0}^*}(x) + \mathcal{L}_{B_{s1}}(x) + \text{H.c.}, \tag{11}
\end{aligned}$$

where summation over isospin indices is understood, $\square = \partial^\mu \partial_\mu$ and $A \overleftrightarrow{\partial} B \equiv A \partial B - B \partial A$. Here, $\vec{\pi} = (\pi_1, \pi_2, \pi_3)$ is the triplet of pions, $\hat{\pi}_B = \pi_1 \tau_1 + \pi_2 \tau_2 + \pi_3 (\tau_3 \cos \varepsilon + I \sin \varepsilon / \sqrt{3})$, $\hat{\pi}_K = \pi_1 \tau_1 + \pi_2 \tau_2 + \pi_3 (\tau_3 \cos \varepsilon + I \sin \varepsilon \sqrt{3})$, $B^{(*)}$ and $K^{(*)}$ are the doublets of pseudoscalar (vector) mesons, B_s^\pm and $B_s^{*\pm}$ are the pseudoscalar and vector bottom-strange mesons, respectively, $V^{*\mu\nu} = \partial^\mu V^{*\nu} - \partial^\nu V^{*\mu}$ is the stress tensor of the vector meson field.

In our convention the isospin-symmetric meson masses of the isomultiplets m_π, m_P, m_V are identified with the masses of the charged partners. The quantities δ_M are the isospin-breaking parameters which are fixed by the difference of masses squared of the charged and neutral members of the isomultiplets as: $\delta_M = m_{M^\pm}^2 - m_{M^0}^2$ and $m_{M^0} \equiv m_{\bar{M}^0}$. The set of mesonic masses is taken from data [33]. From Eq. (11) it is evident that the couplings of π^0 to the B^*B and K^*K mesonic pairs contain two terms — the “dominant” coupling (proportional to $\cos \varepsilon$) and the “suppressed” coupling (proportional to $\sin \varepsilon$). This means that the first coupling survives in the isospin limit, while the second one vanishes.

The free meson propagators are given by the standard expressions

$$i D_M(x-y) = \langle 0 | T M(x) M^\dagger(y) | 0 \rangle = \int \frac{d^4 k}{(2\pi)^4 i} e^{-ik(x-y)} \tilde{D}_M(k) \tag{12}$$

for the scalar (pseudoscalar) fields, where $\tilde{D}_M(k) = (m_M^2 - k^2 - i\epsilon)^{-1}$ and

$$i D_{M^*}^{\mu\nu}(x-y) = \langle 0 | T M^{*\mu}(x) M^{*\nu\dagger}(y) | 0 \rangle = \int \frac{d^4 k}{(2\pi)^4 i} e^{-ik(x-y)} \tilde{D}_{M^*}^{\mu\nu}(k) \tag{13}$$

for the vector (axial) fields, where $\tilde{D}_{M^*}^{\mu\nu}(k) = (-g^{\mu\nu} + k^\mu k^\nu / m_{M^*}^2) (m_{M^*}^2 - k^2 - i\epsilon)^{-1}$. The choice for the strong meson couplings of the Lagrangian (11) will be discussed in Sec.III.

The electromagnetic field is included in the Lagrangian (9) using minimal substitution i.e. each derivative acting on a charged meson field is replaced by the covariant one: $\partial^\mu M^{(*)\pm} \rightarrow (\partial^\mu \mp ieA^\mu) M^{(*)\pm}$. Note, that the strong interaction Lagrangians $\mathcal{L}_{B_{s0}^*}$ and $\mathcal{L}_{B_{s1}}$ should also be modified in order to restore electromagnetic gauge invariance. It proceeds in a way as suggested in Ref. [34] and is extensively used in Refs. [3, 5, 10]. In particular, each charged constituent meson field H^\pm (i.e. $B^{(*)\pm}$ and $K^{(\pm)}$) in $\mathcal{L}_{B_{s0}^*}$ and $\mathcal{L}_{B_{s1}}$ is multiplied by the gauge field exponential (see further details in [3, 5, 10]):

$$H^\pm(y) \rightarrow e^{\mp ieI(y,x,P)} H^\pm(y) \tag{14}$$

where

$$I(x, y, P) = \int_y^x dz_\mu A^\mu(z). \tag{15}$$

For the derivative of $I(x, y, P)$ we use the path-independent prescription suggested in [34] which in turn states that the derivative of $I(x, y, P)$ does not depend on the path P originally used in the definition. The nonminimal substitution (14) is therefore completely equivalent to the minimal prescription. Expanding the exponential $e^{\mp ieI(y,x,P)} H^\pm(y)$ in powers of the electromagnetic field and keeping linear terms like the four-particle coupling $B_{s0}^* B^+ K^- \gamma$ and $B_{s1} B^{*+} K^- \gamma$ we generate the diagrams of Figs.4(c) and 5(c), 6(c), 6(d), respectively.

Finally, we specify the electromagnetic Lagrangian describing the coupling of vector and pseudoscalar mesons to the photon:

$$\begin{aligned}
\mathcal{L}_{VP\gamma}(x) = & \frac{e}{4} F_{\mu\nu}(x) \epsilon^{\mu\nu\alpha\beta} \left(g_{K^*\pm K^\pm\gamma} K_{\alpha\beta}^{*\pm}(x) K^-(x) + g_{K^*0 K^0\gamma} K_{\alpha\beta}^{*0}(x) \bar{K}^0(x) \right. \\
& \left. + g_{B^*\pm B^\pm\gamma} B_{\alpha\beta}^{*\pm}(x) B^-(x) + g_{B^*0 B^0\gamma} B_{\alpha\beta}^{*0}(x) \bar{B}^0(x) \right) + \text{H.c.} \tag{16}
\end{aligned}$$

Here the couplings $g_{VP\gamma}$ can be extracted from the corresponding decay widths $V \rightarrow P + \gamma$. Presently we only have information about the decay width of K^* mesons. Using the expressions for the $K^* \rightarrow K + \gamma$ decay widths

$$\Gamma(K^* \rightarrow K\gamma) = \frac{\alpha}{24} g_{K^* K\gamma}^2 m_{K^*}^3 \left(1 - \frac{m_K^2}{m_{K^*}^2}\right)^3 \quad (17)$$

and the data (central values) for $\Gamma(K^{*\pm} \rightarrow K^\pm \gamma) = 50.29$ keV and $\Gamma(K^{*0} \rightarrow K^0 \gamma) = 116.19$ keV we deduce the coupling constants $g_{K^{*\pm} \rightarrow K^\pm \gamma} = 0.836$ GeV $^{-1}$ and $g_{K^{*0} \rightarrow K^0 \gamma} = -1.267$ GeV $^{-1}$. Note, that in the nonrelativistic SU(3) quark model the couplings $g_{K^{*\pm} \rightarrow K^\pm \gamma}$ and $g_{K^{*0} \rightarrow K^0 \gamma}$ are proportional to the sum of the charges of the constituent quarks: $g_{K^{*\pm} \rightarrow K^\pm \gamma} \sim (e_u + e_s) = 1/3$ and $g_{K^{*0} \rightarrow K^0 \gamma} \sim (e_d + e_s) = -2/3$. This is the reason why the coupling of the neutral kaons is defined (by convention) with a negative sign. Also, the prediction of the nonrelativistic quark model for the ratio $g_{K^{*0} \rightarrow K^0 \gamma}/g_{K^{*\pm} \rightarrow K^\pm \gamma} = -2$ is violated by relativistic corrections. For D mesons the corresponding ratio is in precise agreement with data. In particular, taking the experimental values of $g_{D^{*\pm} \rightarrow D^\pm \gamma} \simeq 0.5$ GeV $^{-1}$ and $g_{D^{*0} \rightarrow D^0 \gamma} \simeq 2.0$ GeV $^{-1}$ (see the discussion in Ref. [35]) we get

$$\frac{g_{D^{*0} \rightarrow D^0 \gamma}}{g_{D^{*\pm} \rightarrow D^\pm \gamma}} = \frac{e_c + e_u}{e_c + e_d} = 4. \quad (18)$$

Therefore, one can expect that for bottom mesons the naive quark model should prediction should also be sufficient:

$$\frac{g_{B^{*0} \rightarrow B^0 \gamma}}{g_{B^{*\pm} \rightarrow B^\pm \gamma}} = \frac{e_b + e_d}{e_b + e_u} = -2. \quad (19)$$

For our numerical estimates we will use typical values with $g_{B^{*\pm} \rightarrow B^\pm \gamma} = 0.5$ GeV $^{-1}$ and $g_{B^{*0} \rightarrow B^0 \gamma} = -1$ GeV $^{-1}$. These couplings correspond to the full width of $B^{*\pm}$ equal to 0.23 keV and of B^{*0} equal to 0.91 keV (as usual we suppose that $B^* \rightarrow B\gamma$ is the dominant mode for the B^* mesons).

III. STRONG AND RADIATIVE DECAYS OF THE B_{s0}^* AND B_{s1} MESONS

A. Matrix elements and decay widths

The matrix elements describing the strong $B_{s0}^* \rightarrow B_s \pi^0$, $B_{s1} \rightarrow B_s^* \pi^0$ and radiative $B_{s0}^* \rightarrow B_s^* \gamma$, $B_{s1} \rightarrow B_s \gamma$ decays are defined as follows

$$M(B_{s0}^*(p) \rightarrow B_s(p')\pi^0(q)) = G_{B_{s0}^* B_s \pi}, \quad (20a)$$

$$M(B_{s1}(p) \rightarrow B_s^*(p')\pi^0(q)) = \epsilon_\mu(p)\epsilon_\nu^*(p') (g^{\mu\nu} G_{B_{s1} B_s^* \pi} - v'^\mu v^\nu F_{B_{s1} B_s^* \pi}), \quad (20b)$$

and

$$M(B_{s0}^*(p) \rightarrow B_s^*(p')\gamma(q)) = e \epsilon_\mu^*(q)\epsilon_\nu^*(p') (g_{\mu\nu} p' q - p'_\mu q_\nu) G_{B_{s0}^* B_s^* \gamma}, \quad (21a)$$

$$M(B_{s1}(p) \rightarrow B_s(p')\gamma(q)) = e \epsilon_\mu(p)\epsilon_\nu^*(q) (g^{\mu\nu} p q - q^\mu p^\nu) G_{B_{s1} B_s \gamma}, \quad (21b)$$

$$\begin{aligned} M(B_{s1}(p) \rightarrow B_s^*(p')\gamma(q)) &= e \varepsilon^{mn\rho\sigma} \epsilon^\alpha(p) \epsilon^{*\mu}(p') \epsilon_\rho^*(q) q_\sigma \left(G_{B_{s1} B_s^* \gamma} g_{\mu n} g_{\alpha m} p q \right. \\ &\quad \left. + F_{B_{s1} B_s^* \gamma} g_{\mu n} p_m q_\alpha + H_{B_{s1} B_s^* \gamma} g_{\alpha m} p_n q_\mu \right), \end{aligned} \quad (21c)$$

$$M(B_{s1}(p) \rightarrow B_{s0}^*(p')\gamma(q)) = e \varepsilon^{\mu\nu\alpha\beta} \epsilon_\mu(p)\epsilon_\nu^*(q) p_\alpha q_\beta G_{B_{s1} B_{s0} \gamma}, \quad (21d)$$

where $v = p/m_{B_{s1}}$ and $v' = p'/m_{B_s^*}$ are the four-velocities of the B_{s1} and B_s^* mesons, $G_{B_{s0}^* B_s \pi}$, $G(F)_{B_{s1} B_s^* \pi}$, $G_{B_{s0}^* B_s^* \gamma}$ and $G_{B_{s1} B_s \gamma}$, $G(F, H)_{B_{s1} B_s^* \gamma}$ and $G_{B_{s1} B_{s0} \gamma}$ are the corresponding effective coupling constants. The coherent sum of all the diagrams in Figs.4-7, contributing to the radiative decays of B_{s0}^* and B_{s1} mesons, is gauge invariant, while the contribution of each diagram is definitely not gauge invariant. As done in Ref. [3], for convenience we split each individual diagram into a gauge-invariant piece and a remainder, which is noninvariant. One can prove that the sum of the noninvariant terms vanishes due to gauge invariance. In the following discussion of the numerical results we will only deal with the gauge-invariant contribution of the separate diagrams of Figs.4-7. In Appendix A we present

the calculational technique for determining the effective couplings entering in the matrix elements of the strong and radiative transitions of B_{s0}^* and B_{s1} mesons.

Using Eqs. (20) and (21) the strong $B_{s0}^* \rightarrow B_s\pi^0$, $B_{s1} \rightarrow B_s^*\pi^0$ and radiative $B_{s0}^* \rightarrow B_s^*\gamma$, $B_{s1} \rightarrow B_s\gamma$, $B_{s1} \rightarrow B_s^*\gamma$, $B_{s1} \rightarrow B_{s0}^*\gamma$ decay widths are calculated according to the expressions:

$$\Gamma(B_{s0}^* \rightarrow B_s\pi^0) = \frac{G_{B_{s0}^* B_s\pi}^2}{8\pi m_{B_{s0}}^2} P_{\pi 1}, \quad (22a)$$

$$\Gamma(B_{s1} \rightarrow B_s^*\pi^0) = \frac{P_{\pi 2}}{12\pi m_{B_{s1}}^2} \left\{ G_{B_{s1} B_s^*\pi}^2 + \frac{1}{2} \left(G_{B_{s1} B_s^*\pi} w - F_{B_{s1} B_s^*\pi}(w^2 - 1) \right)^2 \right\}, \quad (22b)$$

and

$$\Gamma(B_{s0}^* \rightarrow B_s^*\gamma) = \alpha G_{B_{s0}^* B_s^*\gamma}^2 P_{\gamma 1}^3, \quad (23a)$$

$$\Gamma(B_{s1} \rightarrow B_s\gamma) = \frac{\alpha}{3} G_{B_{s1} B_s\gamma}^2 P_{\gamma 2}^3, \quad (23b)$$

$$\Gamma(B_{s1} \rightarrow B_s^*\gamma) = \frac{\alpha}{3} P_{\gamma 3}^5 \left\{ \left(G_{B_{s1} B_s^*\gamma} + F_{B_{s1} B_s^*\gamma} \right)^2 + \frac{m_{B_{s1}}^2}{m_{B_s^*}^2} \left(G_{B_{s1} B_s^*\gamma} + H_{B_{s1} B_s^*\gamma} \right)^2 \right\}, \quad (23c)$$

$$\Gamma(B_{s1} \rightarrow B_{s0}^*\gamma) = \frac{\alpha}{3} G_{B_{s1} B_{s0}^*\gamma}^2 P_{\gamma 4}^3, \quad (23d)$$

where $w = vv' = (m_{B_{s1}}^2 + m_{B_s^*}^2 - m_{\pi^0}^2)/(2m_{B_{s1}}m_{B_s^*})$ and $P_{\pi i}$, $P_{\gamma i}$ are the corresponding three-momenta of the decay products.

Note, the contribution of the effective coupling constant $F_{B_{s1} B_s^*\pi}$ to the $B_{s1} \rightarrow B_s^*\pi^0$ decay width is strongly suppressed. This is because the contribution of the matrix element with $F_{B_{s1} B_s^*\pi}$ is proportional to the suppressed factor $w^2 - 1 \simeq 4 \times 10^{-3}$ with $w \simeq 1$. Therefore, we have

$$\Gamma(B_{s1} \rightarrow B_s^*\pi^0) \simeq \frac{G_{B_{s1} B_s^*\pi}^2}{8\pi m_{B_{s1}}^2} P_{\pi 2} \quad (24)$$

and

$$\frac{\Gamma(B_{s1} \rightarrow B_s^*\pi^0)}{\Gamma(B_{s0}^* \rightarrow B_s\pi^0)} \simeq \frac{P_{\pi 2}}{P_{\pi 1}} \left(\frac{m_{B_{s0}}}{m_{B_{s1}}} \right)^2 \left(\frac{G_{B_{s1} B_s^*\pi}}{G_{B_{s0}^* B_s\pi}} \right)^2. \quad (25)$$

B. Numerical results

First, we discuss the choice for the strong coupling constants in the Lagrangian \mathcal{L}_{str} (9). In Refs. [3, 5] we used the set of strong coupling constants $g_{D_1 D_2 L}$ ($g_{D^* D\pi}$, $g_{D_s D^* K} = g_{D_s K^* D}$ and $g_{D_s^* D K} = g_{D_s^* D^* K^*}$) defined in the charm sector, where index L denotes a light meson, while D_1 and D_2 are the respective charm states. The coupling $g_{D^* D\pi} = 17.9$ was deduced using data for the corresponding strong decay width [36]. The coupling constants $g_{D_s D^* K}$ and $g_{D_s^* D K}$ have been estimated using two different variants of the QCD sum rule approach discussed in Refs. [37, 38], where similar results have been obtained. Both Refs. [37, 38] point to a strong suppression of these constants in comparison to the coupling $g_{D^* D\pi}$. An updated analysis for $g_{D^* D\pi}$ in the context of a QCD sum rule approach gives a result close to data – $g_{D^* D\pi} = 14 \pm 1.5$ [39]. We used the predictions of Ref. [37]: $g_{D^* D_s K} = 2.02$ and $g_{D_s^* D K} = 1.84$. For the unknown parameters $g_{D_s K^* D}$ and $g_{D_s^* D^* K^*}$ we used the approximative relations $g_{D_s K^* D} \simeq g_{D_s D^* K}$ and $g_{D_s^* D^* K^*} \simeq g_{D_s^* D K}$, which can be explained phenomenologically: the first relation – by the universality of the coupling of the D_s meson to $D^* K$ and $K^* D$ mesonic pairs (it is based on exact SU(4) flavor symmetry and we do not expect a substantial violation of this relation due to breaking of the SU(4) symmetry) and the second relation – by the universality of the coupling of the D_s^* meson to two pseudoscalars and two vectors (like for $\rho\pi\pi$ and $\rho\rho\rho$ couplings: $g_{\rho\pi\pi} \simeq g_{\rho\rho\rho} \simeq 6$, and also for $J/\Psi D D$ and $J/\Psi D^* D^*$: $g_{J/\Psi D D} \simeq g_{J/\Psi D^* D^*} \simeq 8$ [40]). For consistency, in the present manuscript we use the set of charmed hadronic couplings predicted by QCD sum rules (central values) with :

$$g_{D^* D\pi} = 14, \quad g_{D_s D^* K} = g_{D_s K^* D} = 2.02, \quad g_{D_s^* D K} = g_{D_s^* D^* K^*} = 1.84. \quad (26)$$

In particular, instead of $g_{D^* D\pi} = 17.9$ we use $g_{D^* D\pi} = 14$. Such a modification does not change the numerical results of Refs. [3, 5], because the contribution of the corresponding diagrams containing the coupling $g_{D^* D\pi}$ is strongly suppressed. A similar picture we also have in the bottom sector (see discussion below).

In order to evaluate the corresponding bottom couplings $g_{B_1 B_2 L}$ we use the arguments of heavy hadron chiral perturbation theory (HHChPT) [41, 42] which relates the bottom and charmed couplings containing the same light meson:

$$g_{B_1 B_2 L} = g_{D_1 D_2 L} \frac{m_B}{m_D} \quad (27)$$

where m_B and m_D are the masses of the bottom and charm mesons identified e.g. with the masses of $m_{B^\pm} = 5.279$ GeV and $m_{D^\pm} = 1.8693$ GeV. In other words, to get the set of bottom meson couplings used in the strong Lagrangian (11) we rescale the corresponding charm meson couplings by a factor $m_{B^\pm}/m_{D^\pm} \simeq 2.82$. In particular, we have:

$$g_{B^* B \pi} = 39.5, \quad g_{B_s B^* K} \simeq g_{B_s K^* B} = 5.70, \quad g_{B_s^* B K} \simeq g_{B_s^* B^* K^*} = 5.19. \quad (28)$$

For the coupling $g_{B_s^* B^* K}$ we have no further input. From a dimensional analysis it should be of order 1 GeV^{-1} . The diagrams 6(e) and 6(f), however, where this coupling enters, are strongly suppressed, and we therefore do not need to have precise knowledge of this constant.

The coupling $g_{K^* K \pi} = 4.61$ is fixed from data on the $K^* K \pi$ decay width [33]. Finally, we fix the couplings $g_{B_{s0}^*}$ and $g_{B_{s1}}$, which are given by Eqs. (6a) and (6b) in terms of the adjustable vertex function. Using the Gaussian vertex function we obtain the result that these couplings are quite stable with respect to a variation of the scale parameter Λ_M . In particular, varying Λ_M from 1 to 2 GeV, we get a range of values for $g_{B_{s0}^*}$ from 27.17 to 23.21 GeV and for $g_{B_{s1}}$ from 25.64 to 22.14 GeV. Note that our predictions for these couplings are in agreement with the results of other theoretical approaches: $g_{B_{s0}^*} = g_{B_{s1}} = 19.6 \pm 5.7$ GeV [light-cone QCD sum rules approach [26]] and $g_{B_{s0}^*} = 23.572$ GeV and $g_{B_{s1}} = 23.442$ GeV [effective chiral approach [20, 21]].

Now we present the numerical results. First, we discuss the results for strong decays. Here the main contribution to the decay width comes, as expected, from the diagrams of Figs.2(a), (b) and 3(a), (b). On the other hand, the contribution of the direct mechanism is comparable to the one of the indirect mechanism (i.e. due to $\eta - \pi^0$ mixing). The contribution of the diagrams in Figs.2(c) and (d) is of order 0.1% of the total contribution to the $G_{B_{s0}^* B_s \pi}$ coupling and the contribution of Figs.3(c) and (d) is of order 1.6% of the total contribution to the $G_{B_{s1} B_s^* \pi}$ coupling. Therefore, the couplings $G_{B_{s0}^* B_s \pi}$ and $G_{B_{s1} B_s^* \pi}$ are not sensitive to a variation of the couplings $g_{B^* B \pi}$, $g_{B_s^* B K}$ and $g_{B_s B^* K}$. They are only sensitive to the values of the couplings $g_{B_s K^* B}$ and $g_{B_s^* B^* K^*}$. The leading-order contributions from the diagrams in Figs.2(a), (b) and 3(a), (b) to the quantities $G_{B_{s0}^* B_s \pi}$ and $G_{B_{s1} B_s^* \pi}$ in terms of the couplings $g_{B_s K^* B}$ and $g_{B_s^* B^* K^*}$ are given by

$$G_{B_{s0}^* B_s \pi} = 65.9 \text{ } g_{B_s K^* B} \text{ MeV}, \quad G_{B_{s1} B_s^* \pi} = 72.3 \text{ } g_{B_s^* B^* K^*} \text{ MeV} \quad (29)$$

for a typical value of the dimensional parameter $\Lambda_M = 1$ GeV. Then, using the specific values of $g_{B_s K^* B} = 5.70$ and $g_{B_s^* B^* K^*} = 5.19$ we get the following predictions for the effective couplings and decay widths:

$$G_{B_{s0}^* B_s \pi} = 375.7(375.6) \text{ MeV}, \quad G_{B_{s1} B_s^* \pi} = 381.1(376.3) \text{ MeV} \quad (30)$$

and

$$\Gamma(B_{s0}^* \rightarrow B_s \pi^0) = 55.2(55.1) \text{ keV}, \quad \Gamma(B_{s1} \rightarrow B_s^* \pi^0) = 57.0(55.6) \text{ keV}. \quad (31)$$

In the brackets we indicate the results of the leading diagrams of Figs.2(a), (b) and 3(a), (b).

The strong decay couplings $G_{B_{s0}^* B_s \pi}$, $G_{B_{s1} B_s^* \pi}$ and the decay widths $\Gamma(B_{s0}^* \rightarrow B_s \pi)$, $\Gamma(B_{s1} \rightarrow B_s^* \pi)$ are practically degenerate, which can also be explained by heavy quark symmetry (HQS), which is a good symmetry for the heavy-light mesons with a bottom quark. Because of the infinitely heavy mass of the bottom quark the spins of the \bar{b} antiquark and the s quark decouple (spin symmetry), and, therefore, the properties of B_{s0}^* and B_{s1} mesons become similar. This issue was also discussed in Refs. [31, 32] in the context of the charm partners (D_{s0}^* and D_{s1}). In particular, it was shown that the corresponding coupling constants and widths are degenerate in the heavy quark limit. In our previous papers we also reproduced the same result. Moreover, for finite charmed meson masses the decay characteristics are nearly degenerate:

$$G_{D_{s0}^* D_s \pi} = 145.4 \text{ MeV}, \quad G_{D_{s1} D_s^* \pi} = 160.2 \text{ MeV} \quad (32)$$

and

$$\Gamma(D_{s0}^* \rightarrow D_s \pi^0) = 46.7 \text{ keV}, \quad \Gamma(D_{s1} \rightarrow D_s^* \pi^0) = 50.1 \text{ keV}. \quad (33)$$

The next point is a check of the flavor content of HQS. In our molecular approach the leading contributions to the couplings $G_{H_{s0}^* H_s \pi}$ and $G_{H_{s1} H_s^* \pi}$, where $H = D$ or B , are defined by the pairs of diagrams in Figs.2(a,b) and 3(a,b), respectively:

$$G_{H_{s0}^* H_s \pi} = g_{H_{s0}^*} g_{K^* K \pi} g_{H_s H K^*} I_{KK^* H}, \quad (34a)$$

$$G_{H_{s1} H_s^* \pi} = g_{H_{s1}} g_{K^* K \pi} g_{H_s^* H^* K^*} I_{KK^* H^*}, \quad (34b)$$

where $I_{KK^* H}$ and $I_{KK^* H^*}$ are the structure integrals which are of order $O(1/m_Q)$ in the inverse heavy quark mass expansion $-1/m_Q$. The hadronic couplings scale as:

$$g_{H_{s0}^*} \sim O(m_Q), \quad g_{H_{s1}} \sim O(m_Q), \quad g_{K^* K \pi} \sim O(1), \quad g_{H_s H K^*} \sim O(m_Q), \quad g_{H_s^* H^* K^*} \sim O(m_Q). \quad (35)$$

Therefore, the strong couplings $G_{H_{s0}^* H_s \pi}$ and $G_{H_{s1} H_s^* \pi}$ scale as: $G_{H_{s0}^* H_s \pi} \sim O(m_Q)$ and $G_{H_{s1} H_s^* \pi} \sim O(m_Q)$. For this scaling behavior the following relations result:

$$\frac{G_{B_{s0}^* B_s \pi}}{G_{D_{s0}^* D_s \pi}} \sim \frac{m_b}{m_c}, \quad \frac{G_{B_{s1} B_s^* \pi}}{G_{D_{s1} D_s^* \pi}} \sim \frac{m_b}{m_c}. \quad (36)$$

With our results [see Eqs. (30) and (32)] we conclude that the constraints (36) are fulfilled very well.

In Table I we present our results for the decay widths $\Gamma(B_{s0}^* \rightarrow B_s \pi^0)$ and $\Gamma(B_{s1} \rightarrow B_s^* \pi^0)$ including a variation of the scale parameter Λ_M from 1 to 2 GeV (an increase of Λ_M leads to an increase of the widths) and compare them with known theoretical predictions [16, 20, 21, 27]. Our results for the decay widths are larger in comparison to previous approaches [16, 20, 21, 27] due to inclusion of the direct isospin-violating transitions $B_{s0}^* \rightarrow B_s \pi^0$ and $B_{s1} \rightarrow B_s^* \pi^0$.

Now we turn to the discussion of the radiative decays $B_{s0}^* \rightarrow B_s^* \gamma$ and $B_{s1} \rightarrow B_s \gamma$. The main contribution to the decay characteristics of the $B_{s0}^* \rightarrow B_s^* \gamma$ and $B_{s1} \rightarrow B_s \gamma$ decays comes, as expected, from the diagrams of Figs.4(a) and 5(a). Our results for the effective coupling constants and decay widths for a typical value of $\Lambda_M = 1$ GeV are:

$$G_{B_{s0}^* B_s^* \gamma} = 0.122 \text{ GeV}^{-1}, \quad G_{B_{s1} B_s \gamma} = 0.115 \text{ GeV}^{-1} \quad (37)$$

and

$$\Gamma(B_{s0}^* \rightarrow B_s^* \gamma) = 3.07 \text{ keV}, \quad \Gamma(B_{s1} \rightarrow B_s \gamma) = 2.01 \text{ keV}. \quad (38)$$

In Table II we summarize our results for the radiative decay widths including a variation of the scale parameter Λ_M from 1 to 2 GeV (an increase of Λ_M leads to a larger value for the width). In comparison, we also display the predictions of other theoretical approaches [16, 23, 28]. The lower limit of the QCD sum rule results [28] is consistent with our predictions. In our opinion the predictions of [16, 23] are overestimated. In particular, applying HQS (spin symmetry) we can relate the corresponding radiative coupling constants of the same flavor as

$$G_{D_{s0}^* D_s^* \gamma} = G_{D_{s1} D_s \gamma}, \quad G_{B_{s0}^* B_s^* \gamma} = G_{B_{s1} B_s \gamma}. \quad (39)$$

The same relation was derived previously in HHChPT [32] in the charm sector. Now we perform the same exercise as done for the strong couplings in order to relate the radiative couplings of different flavors. The leading contributions to the couplings $G_{H_{s0}^* H_s^* \gamma}$ and $G_{H_{s1} H_s \gamma}$, are defined by the pairs of diagrams in Figs.4(a) and 5(a), respectively:

$$G_{H_{s0}^* H_s^* \gamma} = g_{H_{s0}^*} g_{K K \gamma} g_{H_s H K} I_{KKH}, \quad (40a)$$

$$G_{H_{s1} H_s \gamma} = g_{H_{s1}} g_{K K \gamma} g_{H_s H^* K} I_{KKH^*}, \quad (40b)$$

where I_{KKH} and I_{KKH^*} are the structure integrals which are of order $O(1/m_Q^2)$. The couplings $g_{K K \gamma}$, $g_{H_s H K}$ and $g_{H_s H^* K}$ scale as: $g_{K K \gamma} \sim O(1)$, $g_{H_s H K} \sim O(m_Q)$ and $g_{H_s H^* K} \sim O(m_Q)$. Therefore, the radiative couplings $G_{H_{s0}^* H_s^* \gamma}$ and $G_{H_{s1} H_s \gamma}$ are insensitive to the flavor of the heavy quark/meson: $G_{H_{s0}^* H_s^* \gamma} \sim O(1)$ and $G_{H_{s1} H_s \gamma} \sim O(1)$. Finally, the radiative couplings obey both spin and flavor symmetry in the heavy quark limit and we arrive at the constraint:

$$G_{D_{s0}^* D_s^* \gamma} = G_{D_{s1} D_s \gamma} = G_{B_{s0}^* B_s^* \gamma} = G_{B_{s1} B_s \gamma}. \quad (41)$$

Recalling the results for the radiative decay constants of charmed mesons [3, 5]

$$G_{D_{s0}^* D_s^* \gamma} = 0.093 \text{ GeV}^{-1}, \quad G_{D_{s1} D_s \gamma} = 0.106 \text{ GeV}^{-1} \quad (42)$$

we conclude that relation (41) is approximately fulfilled by our results, which are obtained for finite physical masses of the heavy mesons. The constraint (41) can also be used to deduce relations between the corresponding decay widths:

$$\frac{\Gamma(D_{s1} \rightarrow D_s \gamma)}{\Gamma(D_{s0}^* \rightarrow D_s^* \gamma)} = \frac{1}{3} \left(\frac{m_{D_{s1}}^2 - m_{D_s}^2}{m_{D_{s0}}^2 - m_{D_s^*}^2} \right)^3 \left(\frac{m_{D_{s0}}^*}{m_{D_{s1}}} \right)^3 \simeq 3.80, \quad (43a)$$

$$\frac{\Gamma(B_{s1} \rightarrow B_s \gamma)}{\Gamma(B_{s0}^* \rightarrow B_s^* \gamma)} = \frac{1}{3} \left(\frac{m_{B_{s1}}^2 - m_{B_s}^2}{m_{B_{s0}}^2 - m_{B_s^*}^2} \right)^3 \left(\frac{m_{B_{s0}}^*}{m_{B_{s1}}} \right)^3 \simeq 0.74, \quad (43b)$$

and

$$\frac{\Gamma(B_{s0}^* \rightarrow B_s^* \gamma)}{\Gamma(D_{s0}^* \rightarrow D_s^* \gamma)} = \left(\frac{m_{B_{s0}}^2 - m_{B_s^*}^2}{m_{D_{s0}}^2 - m_{D_s^*}^2} \right)^3 \left(\frac{m_{D_{s0}}^*}{m_{B_{s0}}} \right)^3 \simeq 3.74, \quad (43c)$$

$$\frac{\Gamma(B_{s1} \rightarrow B_s \gamma)}{\Gamma(D_{s1} \rightarrow D_s \gamma)} = \left(\frac{m_{B_{s1}}^2 - m_{B_s}^2}{m_{D_{s1}}^2 - m_{D_s}^2} \right)^3 \left(\frac{m_{D_{s1}}}{m_{B_{s1}}} \right)^3 \simeq 0.73. \quad (43d)$$

Relation (43a) is confirmed by the full analysis done in our framework and in other theoretical approaches (see compilation of the results in Refs. [3, 5]). E.g. the relation explains why most of the approaches predict that the decay width $\Gamma(D_{s1} \rightarrow D_s \gamma)$ is approximately 3–5 times larger than $\Gamma(D_{s0}^* \rightarrow D_s^* \gamma)$. The other relations (43b)–(43d) help to give predictions for the decay widths of the bottom partners. In particular, we arrive at the conclusion that our full predictions for $\Gamma(B_{s0}^* \rightarrow B_s^* \gamma)$ and $\Gamma(B_{s1} \rightarrow B_s \gamma)$ – a few keV – are well justified.

Now we discuss the ratios of radiative and strong decay modes. For both systems, B_{s0}^* and B_{s1} , we predict small ratios:

$$\begin{aligned} R_{B_{s0}^*} &= \frac{B_{s0}^* \rightarrow B_s^* \gamma}{B_{s0}^* \rightarrow B_s \pi} \simeq 0.05, \\ R_{B_{s1}} &= \frac{B_{s1} \rightarrow B_s \gamma}{B_{s1} \rightarrow B_s^* \pi} \simeq 0.03. \end{aligned} \quad (44a)$$

Note that similar results we also obtained in the charm sector: $R_{D_{s0}^*} = 0.01$ and $R_{D_{s1}} = 0.05$. The predicted ratio $R_{D_{s0}^*}$ is consistent with the present experimental limit $R_{D_{s0}^*} < 0.059$, while the ratio $R_{D_{s1}}$ is smaller than the result quoted by the Particle Data Group $R_{D_{s1}} = 0.38 \pm 0.05$ [33]. We consider this experimental result as preliminary, since it is not clear why the ratio for the axial state D_{s1} is much larger than for the scalar state D_{s0}^* . At this point more precise data on the strong and radiative decays of the D_{s1} meson and their ratio would be very helpful.

Finally, we give the predictions for the other two radiative decay modes of B_{s1} mesons – $B_{s1} \rightarrow B_s^* \gamma$ and $B_{s1} \rightarrow B_{s0}^* \gamma$. These decay amplitudes are generated by the anomalous couplings of two vectors and one pseudoscalar and one can expect that they are suppressed. Moreover, there is an additional mechanism for their suppression. The leading diagrams in the process $B_{s1} \rightarrow B_s^* \gamma$ are the ones of Figs.6(a) and (b). The separate contribution of the diagrams in Figs.6(c)–(f) to the corresponding decay width is of order 1%. The diagrams of Figs.6(a) and Figs.6(b) are subtracted from each other because of the opposite sign of the anomalous couplings $g_{K^* \pm \rightarrow K^\pm \gamma} = 0.836 \text{ GeV}^{-1}$ and $g_{K^* 0 \rightarrow K^0 \gamma} = -1.267 \text{ GeV}^{-1}$. In the case of the $B_{s1} \rightarrow B_{s0}^* \gamma$ decay we only have two diagrams contributing to the matrix element. Again, due to the opposite sign of the anomalous couplings $g_{B^* \pm \rightarrow B^\pm \gamma} = 0.5 \text{ GeV}^{-1}$ and $g_{B^* 0 \rightarrow B^0 \gamma} = -1 \text{ GeV}^{-1}$ their total contribution is given by the difference of the individual contributions. Finally, as a full result we get values of 0.04 to 0.18 keV for the decay width of $B_{s1} \rightarrow B_s^* \gamma$ including a variation of the model parameter Λ from 1 to 2 GeV. The result for the decay width of $B_{s1} \rightarrow B_{s0}^* \gamma$ is stable with respect to a variation of the model parameter Λ in the same range and is equal to 0.022 keV. We also present the result for $\Gamma(B_{s1} \rightarrow B_{s0}^* \gamma)$ in terms of the couplings $g_{B^* \pm \rightarrow B^\pm \gamma}$ and $g_{B^* 0 \rightarrow B^0 \gamma}$:

$$\Gamma(B_{s1} \rightarrow B_{s0}^* \gamma) = [(g_{B^* \pm \rightarrow B^\pm \gamma} + g_{B^* 0 \rightarrow B^0 \gamma}) \times 1 \text{ GeV}]^2 0.088 \text{ keV}. \quad (45)$$

Recently, these radiative decay widths have also been estimated using light-cone QCD sum rules [28]: $\Gamma(B_{s1} \rightarrow B_s^* \gamma) = 0.3 - 6.1 \text{ keV}$ and $\Gamma(B_{s1} \rightarrow B_{s0}^* \gamma) = 0.002 - 0.008 \text{ keV}$. The decay width $\Gamma(B_{s1} \rightarrow B_{s0}^* \gamma)$ is definitely strongly suppressed in both approaches. The decay width $\Gamma(B_{s1} \rightarrow B_s^* \gamma)$ predicted in [28] is also smaller in comparison to the other two modes $B_{s0}^* \rightarrow B_s^* \gamma$ and $B_{s1} \rightarrow B_s \gamma$ (see Table II).

IV. SUMMARY

In this paper we studied the new bottom-strange mesons $B_{s0}^*(5725)$ and $B_{s1}(5778)$ in the hadronic molecule interpretation, i.e., we considered them as bound states of BK and B^*K mesons using a phenomenological Lagrangian approach. Our approach is based on the compositeness condition with $Z = 0$ (the renormalization constant of the molecular state equals zero). This condition is crucial for weakly bound states. The compositeness condition is a self-consistent tool to evaluate for a hadronic molecule, once the mass of the bound state is fixed, its coupling to the intermediate hadronic state, which in turn feeds the accessible final states. Once the further hadronic couplings to generate the final states are known, this approach is fairly model-independent in the results for the observable decay modes. Furthermore, the Lagrangian method implied by the compositeness condition allows a fully Lorentz and gauge-invariant treatment of the problem.

We calculated the strong $B_{s0}^* \rightarrow B_s\pi^0$, $B_{s1} \rightarrow B_s^*\pi^0$ and radiative $B_{s0}^* \rightarrow B_s^*\gamma$, $B_{s1} \rightarrow B_s\gamma$, $B_{s1} \rightarrow B_s^*\gamma$, $B_{s1} \rightarrow B_{s0}^*\gamma$ decays. A new impact of the BK and B^*K molecular structures of the $B_{s0}^*(5725)$ and $B_{s1}(5778)$ mesons is that the presence of $u(d)$ quarks in the $B^{(*)}$ and K meson loops gives rise to direct strong isospin-violating transitions $B_{s0}^* \rightarrow B_s\pi^0$ and $B_{s1} \rightarrow B_s^*\pi^0$ in addition to the decay mechanism induced by $\eta - \pi^0$ mixing. We showed that the direct transition is comparable with the $\eta - \pi^0$ mixing transition. As a consequence, the presence of the direct mode makes our predictions larger than the ones of previous approaches. In the case of the radiative decays $B_{s0}^* \rightarrow B_s^*\gamma$ and $B_{s1} \rightarrow B_s\gamma$, our results are considerably smaller than in previous calculations. We also gave predictions for the anomalous decays $B_{s1} \rightarrow B_s^*\gamma$ and $B_{s1} \rightarrow B_{s0}^*\gamma$: their decay widths are suppressed in comparison to the leading radiative modes $B_{s0}^* \rightarrow B_s^*\gamma$ and $B_{s1} \rightarrow B_s\gamma$.

In series of papers [3]-[5] we already studied in detail strong, electromagnetic and weak decays of D_{s0}^* and D_{s1} states, as a consequence of their possible molecular structure. At present we do not think that the structure issue concerning the D_{s0}^* and D_{s1} mesons is settled yet, in particular because the mass and the narrowness of these states cannot be easily explained in the context of the standard $c\bar{s}$ picture [1, 2]. A further direct consequence and analogy of possible hadronic molecules in the D_s sector is also found in the B_s system. If the B_{s0}^* and B_{s1} mesons can possibly be experimentally established near the predicted mass values, then, because of their closeness to the BK and BK^* thresholds, they are clear candidates for hadronic molecules. In the present approach we give clear predictions for the possible strong and radiative decay modes of B_{s0}^* and B_{s1} mesons accessible by experiment. Strong experimental deviations from our results would discard the molecular interpretation of these states. We hope that our results will be useful for future experiments, where B_{s0}^* and B_{s1} could possibly be detected.

Acknowledgments

This work was supported by the DFG under Contract Nos. FA67/31-1 and GRK683. This research is also part of the EU Integrated Infrastructure Initiative Hadronphysics project under Contract No. RII3-CT-2004-506078 and the President Grant of Russia “Scientific Schools” No. 871.2008.2

APPENDIX A: EFFECTIVE COUPLINGS FOR STRONG AND RADIATIVE TRANSITIONS OF B_{s0}^* AND B_{s1} MESONS.

Here we discuss the calculational technique of the matrix elements of strong and radiative transitions of B_{s0}^* and B_{s1} mesons.

As an example for the calculation of diagrams presented in Figs.1-7 we consider a generic loop integral containing a product of n virtual momenta $k_{\mu_1} \cdots k_{\mu_n}$, three meson propagators with masses m_1 , m_2 and m_3 and the correlation function of the molecular state (B_{s0}^* or B_{s1} meson)

$$I_{\mu_1 \cdots \mu_n}(p, p') = \int \frac{d^4k}{\pi^2 i} \tilde{\Phi}(-k^2) \frac{k_{\mu_1} \cdots k_{\mu_n}}{(m_1^2 - (k+p)^2)(m_2^2 - (k+p')^2)(m_3^2 - k^2)}. \quad (\text{A1})$$

The three main ingredients are

- use of the Laplace transform of the vertex function

$$\tilde{\Phi}(-z) = \int_0^\infty ds \tilde{\Phi}_L(s) e^{sz},$$

which is useful to proceed with vertex functions of any functional form,

- the α -transform of the denominator

$$\frac{1}{m_i^2 - k_i^2} = \int_0^\infty d\alpha e^{-\alpha(m_i^2 - k_i^2)},$$

- the differential representation of the numerator

$$k_{\mu_i} e^{kR} = \frac{\partial}{\partial R^{\mu_i}} e^{kR},$$

where R is a linear combination of the external momenta.

The calculation of the transition form factors amounts to a one-loop integration. Integration over the loop momentum is done analytically. One ends up with the integrals over α Feynman parameters which are not difficult to evaluate numerically. All calculations are done by using computer programs written in FORM [43] and in FORTRAN for numerical evaluations. Also, for transparency we give explicit expressions for the leading contributions to the effective couplings defining the structure of the matrix elements of strong and radiative decays of B_{s0}^* and B_{s1} mesons.

1. Decay $B_{s0}^* \rightarrow B_s \pi^0$.

The leading contribution to the coupling constant $G_{B_{s0}^* B_s \pi}$ coming from the diagrams in Figs.2(a) and 2(b) is defined by

$$G_{B_{s0}^* B_s \pi} = \frac{1}{16\pi^2} g_{B_{s0}^*} g_{K^* K \pi} g_{B_s B K^*} I_{B_{s0}^* B_s \pi}. \quad (\text{A2})$$

Here $I_{B_{s0}^* B_s \pi}$ is the structure integral

$$\begin{aligned}
I_{B_{s0}^* B_s \pi} &= \sum_{i=1}^5 I_{B_{s0}^* B_s \pi}^i, \\
I_{B_{s0}^* B_s \pi}^1 &= \int_0^\infty \int_0^\infty \int_0^\infty \frac{d\alpha_1 d\alpha_2 d\alpha_3}{\Delta_1^2} \exp(A_1) N_1, \\
I_{B_{s0}^* B_s \pi}^2 &= \int_0^\infty \int_0^\infty \int_0^\infty \frac{d\alpha_1 d\alpha_2}{\Delta_2^2} \exp(A_2) N_2, \\
I_{B_{s0}^* B_s \pi}^3 &= \int_0^\infty \int_0^\infty \int_0^\infty \frac{d\alpha_1 d\alpha_2}{\Delta_3^2} \exp(A_3) N_3, \\
I_{B_{s0}^* B_s \pi}^4 &= \int_0^\infty \int_0^\infty \int_0^\infty \frac{d\alpha_1 d\alpha_2}{\Delta_4^2} \exp(A_4) N_4, \\
I_{B_{s0}^* B_s \pi}^5 &= \int_0^\infty \int_0^\infty \frac{d\alpha_1}{\Delta_5^2} \exp(A_5) N_5,
\end{aligned} \tag{A3}$$

where we introduce the set of notations:

$$\Delta_1 = 1 + \alpha_{123}, \quad \Delta_2 = \Delta_3 = \Delta_4 = 1 + \alpha_{12}, \quad \Delta_5 = 1 + \alpha_1,$$

$$\begin{aligned}
A_1 &= -\alpha_1 \mu_B^2 - \alpha_2 \mu_{K^*}^2 - \alpha_3 \mu_K^2 - \mu_{B_{s0}^*}^2 w_{BK} w_{KB} + \frac{1}{\Delta_1} \left(\mu_{B_{s0}^*}^2 \alpha_{1KB} \alpha_{3BK} + \mu_{B_s}^2 \alpha_{1KB} \alpha_2 + \mu_\pi^2 \alpha_{3BK} \alpha_2 \right), \\
A_2 &= -\alpha_1 \mu_B^2 - \alpha_2 \mu_{K^*}^2 - \mu_{B_{s0}^*}^2 w_{BK} w_{KB} + \frac{1}{\Delta_2} \left(\mu_{B_{s0}^*}^2 \alpha_{1KB} w_{BK} + \mu_{B_s}^2 \alpha_{1KB} \alpha_2 + \mu_\pi^2 w_{BK} \alpha_2 \right), \\
A_3 &= -\alpha_1 \mu_{K^*}^2 - \alpha_2 \mu_K^2 - \mu_{B_{s0}^*}^2 w_{BK} w_{KB} + \frac{1}{\Delta_3} \left(\mu_{B_{s0}^*}^2 \alpha_{2BK} w_{KB} + \mu_{B_s}^2 w_{KB} \alpha_1 + \mu_\pi^2 \alpha_{2BK} \alpha_1 \right), \\
A_4 &= -\alpha_1 \mu_B^2 - \alpha_2 \mu_K^2 - \mu_{B_{s0}^*}^2 w_{BK} w_{KB} + \frac{1}{\Delta_4} \mu_{B_{s0}^*}^2 \alpha_{1KB} \alpha_{2BK}, \\
A_5 &= -\alpha_1 \mu_{K^*}^2 - \mu_{B_{s0}^*}^2 w_{BK} w_{KB} + \frac{1}{\Delta_5} \left(\mu_{B_{s0}^*}^2 w_{BK} w_{KB} + \mu_{B_s}^2 w_{KB} \alpha_1 + \mu_\pi^2 w_{BK} \alpha_1 \right), \\
N_1 &= \mu_B^2 + \mu_K - 2\mu_{B_{s0}^*}^2 + \mu_{B_s}^2 + \mu_\pi^2 - \mu_{K^*}^2 + \frac{\mu_K^2 - \mu_\pi^2}{\mu_{K^*}^2} (\mu_{B_s}^2 - \mu_B^2), \\
N_2 &= 1 + \frac{\mu_{B_s}^2 - \mu_B^2}{\mu_{K^*}^2}, \\
N_3 &= -1 + \frac{\mu_K^2 - \mu_\pi^2}{\mu_{K^*}^2}, \\
N_4 &= 1, \\
N_5 &= -\frac{1}{\mu_{K^*}^2},
\end{aligned}$$

$$w_{M_1 M_2} = \frac{m_{M_1} m_{M_2}}{m_{M_1} + m_{M_2}}, \quad \alpha_{123} = \alpha_1 + \alpha_2 + \alpha_3, \quad \alpha_{12} = \alpha_1 + \alpha_2, \quad \alpha_{i M_1 M_2} = \alpha_i + w_{M_1 M_2}, \quad \mu_M = \frac{m_M}{\Lambda}.$$

2. Decay $B_{s1} \rightarrow B_s^* \pi^0$.

The leading contributions to the coupling constants $G_{B_{s1}^* B_s^* \pi}$ and $F_{B_{s1}^* B_s^* \pi}$ coming from the diagrams in Figs.3(a) and 3(b) are defined by

$$G_{B_{s1}^* B_s^* \pi} = \frac{1}{16\pi^2} g_{B_{s1}} g_{K^* K \pi} g_{B_s^* B^* K^*} I_{B_{s1}^* B_s^* \pi}^G \quad (\text{A4})$$

and

$$F_{B_{s1}^* B_s^* \pi} = \frac{1}{16\pi^2} g_{B_{s1}} g_{K^* K \pi} g_{B_s^* B^* K^*} I_{B_{s1}^* B_s^* \pi}^F. \quad (\text{A5})$$

Here $I_{B_{s1}^* B_s^* \pi}^G$ and $I_{B_{s1}^* B_s^* \pi}^F$ are the structure integrals

$$\begin{aligned} I_{B_{s1}^* B_s^* \pi}^G &= \sum_{i=1}^5 I_{B_{s1}^* B_s^* \pi}^{G,i}, \\ I_{B_{s1}^* B_s^* \pi}^{G,1} &= \int_0^\infty \int_0^\infty \int_0^\infty \frac{d\alpha_1 d\alpha_2 d\alpha_3}{\Delta_1^2} \exp(A_1^G) N_1^G, \\ I_{B_{s1}^* B_s^* \pi}^{G,2} &= \int_0^\infty \int_0^\infty \int_0^\infty \frac{d\alpha_1 d\alpha_2}{\Delta_2^2} \exp(A_2^G) N_2^G, \\ I_{B_{s1}^* B_s^* \pi}^{G,3} &= \int_0^\infty \int_0^\infty \int_0^\infty \frac{d\alpha_1 d\alpha_2}{\Delta_3^2} \exp(A_3^G) N_3^G, \\ I_{B_{s1}^* B_s^* \pi}^{G,4} &= \int_0^\infty \int_0^\infty \int_0^\infty \frac{d\alpha_1 d\alpha_2}{\Delta_4^2} \exp(A_4^G) N_4^G, \\ I_{B_{s1}^* B_s^* \pi}^{G,5} &= \int_0^\infty \int_0^\infty \frac{d\alpha_1}{\Delta_5^2} \exp(A_5^G) N_5^G, \end{aligned} \quad (\text{A6})$$

and

$$\begin{aligned} I_{B_{s1}^* B_s^* \pi}^F &= \sum_{i=1}^2 I_{B_{s1}^* B_s^* \pi}^{F,i}, \\ I_{B_{s1}^* B_s^* \pi}^{F,1} &= \int_0^\infty \int_0^\infty \int_0^\infty \frac{d\alpha_1 d\alpha_2 d\alpha_3}{\Delta_1^2} \exp(A_1^F) N_1^F, \\ I_{B_{s1}^* B_s^* \pi}^{F,2} &= \int_0^\infty \int_0^\infty \int_0^\infty \frac{d\alpha_1 d\alpha_2}{\Delta_2^2} \exp(A_2^F) N_2^F, \end{aligned} \quad (\text{A7})$$

where we introduce the set of notations:

$$\begin{aligned} A_1^G &= A_1^F = -\alpha_1 \mu_{K^*}^2 - \alpha_2 \mu_K^2 - \alpha_3 \mu_{B^*}^2 - \mu_{B_{s1}}^2 w_{B^* K} w_{K B^*} \frac{1}{\Delta_1} \left(\mu_{D_{s1}}^2 \alpha_{1 K B^*} \alpha_{3 B^* K} + \mu_{B_s}^2 \alpha_{1 K B^*} \alpha_2 + \mu_\pi^2 \alpha_{3 B^* K} \alpha_2 \right), \\ A_2^G &= A_2^F = -\alpha_1 \mu_B^2 - \alpha_2 \mu_{K^*}^2 - \mu_{B_{s1}}^2 w_{B^* K} w_{K B^*} + \frac{1}{\Delta_2} \left(\mu_{B_{s1}}^2 \alpha_{1 K B^*} w_{B^* K} + \mu_{B_s}^2 \alpha_{1 K B^*} \alpha_2 + \mu_\pi^2 w_{B^* K} \alpha_2 \right), \\ A_3^G &= -\alpha_1 \mu_{K^*}^2 - \alpha_1 \mu_K^2 - \mu_{B_{s1}}^2 w_{B^* K} w_{K B^*} + \frac{1}{\Delta_3} \left(\mu_{B_{s1}}^2 \alpha_{2 B^* K} w_{K B^*} + \mu_{B_s}^2 w_{K B^*} \alpha_1 + \mu_\pi^2 \alpha_{2 B^* K} \alpha_1 \right), \\ A_4^G &= -\alpha_1 \mu_B^2 - \alpha_1 \mu_K^2 - \mu_{B_{s1}}^2 w_{B^* K} w_{K B^*} + \frac{1}{\Delta_4} \mu_{B_{s1}}^2 \alpha_{1 K B^*} \alpha_{2 B^* K}, \\ A_5^G &= -\alpha_1 \mu_{K^*}^2 - \mu_{B_{s1}}^2 w_{B^* K} w_{K B^*} + \frac{1}{\Delta_5} \left(\mu_{B_{s1}}^2 w_{B^* K} w_{K B^*} + \mu_{B_s}^2 w_{K B^*} \alpha_1 + \mu_\pi^2 w_{B^* K} \alpha_1 \right), \end{aligned}$$

$$\begin{aligned}
N_1^G &= 2\mu_{B_{s1}}^2 - \mu_{B_s}^2 - \mu_{B^*}^2 + \mu_{K^*}^2 - \mu_K^2 + \frac{\mu_K^2}{\mu_{K^*}^2}(\mu_{B^*}^2 - \mu_{B_s}^2) - \frac{\mu_{K^*}^2 - \mu_K^2}{2\mu_{B^*}^2\mu_{K^*}^2\Delta_1}(\mu_{B^*}^2 + \mu_{K^*}^2 - \mu_{B_s}^2), \\
N_2^G &= \frac{\mu_{B_s}^2 + \mu_{K^*}^2 - \mu_{B^*}^2}{\mu_{K^*}^2} - \frac{\mu_{B^*}^2 + \mu_{K^*}^2 - \mu_{B_s}^2}{2\mu_{B^*}^2\mu_{K^*}^2\Delta_2}, \\
N_3^G &= -1 + \frac{1}{2\mu_{B^*}^2\Delta_3}, \\
N_4^G &= \frac{\mu_{K^*}^2 - \mu_K^2}{\mu_{K^*}^2}, \\
N_5^G &= \frac{1}{\mu_{K^*}^2}, \\
N_1^F &= \frac{\mu_{B_{s1}}\mu_{B_s}^*}{\Delta_1} \left(4(\alpha_{13} + w_{KB^*}) + \frac{\alpha_3}{\Delta_1} \frac{\alpha_{13} + w_{KB^*}}{\mu_{B^*}^2\mu_{K^*}^2} (\mu_{B^*}^2 + \mu_{K^*}^2 - \mu_{B_s}^2)(\mu_{K^*}^2 - \mu_K^2) \right. \\
&\quad \left. - \alpha_3 \frac{(\mu_{K^*}^2 + \mu_K^2)(\mu_{B_s}^2 - \mu_{K^*}^2) + \mu_{B^*}^2(3\mu_{K^*}^2 - \mu_K^2)}{\mu_{B^*}^2\mu_{K^*}^2} \right) \\
N_2^F &= -\frac{\alpha_3}{\Delta_2} \frac{\mu_{B_{s1}}\mu_{B_s}^*}{\mu_{B^*}^2\mu_{K^*}^2} (\mu_{B^*}^2 + \mu_{K^*}^2 - \mu_{B_s}^2) \left(1 - \frac{\alpha_{13} + w_{KB^*}}{\Delta_2} \right).
\end{aligned}$$

3. Decay $B_{s0}^* \rightarrow B_s^*\gamma$.

The leading contribution to the coupling constant $G_{B_{s0}B_s^*\gamma}$ comes from the diagram in Fig.4(a) and is defined by

$$G_{B_{s0}^*B_s^*\gamma} = \frac{1}{16\pi^2\Lambda^2} g_{B_{s0}^*} g_{B_s^*B_K} I_{B_{s0}^*B_s^*\gamma}, \quad (\text{A8})$$

where $I_{B_{s0}^*B_s^*\gamma}$ is the structure integral

$$I_{B_{s0}^*B_s^*\gamma} = \int_0^\infty \int_0^\infty \int_0^\infty \frac{d\alpha_1 d\alpha_2 d\alpha_3}{\Delta_1^4} \exp(B_1) \alpha_{1BK} \alpha_{3KB}, \quad (\text{A9})$$

where

$$B_1 = -\alpha_{12}\mu_K^2 - \alpha_3\mu_B^2 - \mu_{B_{s0}}^2 w_{BK} w_{KB} + \frac{\alpha_{3KB}}{\Delta_1} (\mu_{B_{s0}}^2 \alpha_{1BK} + \mu_{B_s}^2 \alpha_2). \quad (\text{A10})$$

4. Decay $B_{s1}^* \rightarrow B_s\gamma$.

The leading contribution to the coupling constant $G_{B_{s1}B_s\gamma}$ is due to the diagram in Fig.5(a) and is defined by

$$G_{B_{s1}B_s\gamma} = \frac{1}{16\pi^2\Lambda^2} g_{B_{s1}} g_{B_s B^{*K}} I_{B_{s1}B_s\gamma}, \quad (\text{A11})$$

where $I_{B_{s1}B_s\gamma}$ is the structure integral

$$I_{B_{s1}B_s\gamma} = \int_0^\infty \int_0^\infty \int_0^\infty \frac{d\alpha_1 d\alpha_2 d\alpha_3}{\Delta_1^3} \exp(B_2) \alpha_{3KB^*} \left(4 - \frac{2\alpha_1}{\Delta_1} \left(1 + \frac{\mu_{D_s}^2 - \mu_K^2}{\mu_{D_s^*}^2} \right) \right), \quad (\text{A12})$$

where

$$B_2 = -\alpha_{12}\mu_K^2 - \alpha_3\mu_{B^*}^2 - \mu_{B_{s1}}^2 w_{B^{*K}} w_{KB^*} + \frac{\alpha_{3KB^*}}{\Delta_1} (\mu_{B_{s0}}^2 \alpha_{1B^{*K}} + \mu_{B_s}^2 \alpha_2). \quad (\text{A13})$$

5. Decay $B_{s1}^* \rightarrow B_s^* \gamma$.

The leading contributions to the coupling constant $G_{B_{s1}B_s^*\gamma}$, $F_{B_{s1}B_s^*\gamma}$ and $H_{B_{s1}B_s^*\gamma}$ coming from the diagrams in Figs.6(a) and (b) are defined by

$$R_{B_{s1}B_s^*\gamma} = \frac{1}{16\pi^2 \Lambda^2} g_{B_s^* B^* K^*} g_{B_{s1}} (g_{K^* \pm K^\pm \gamma} + g_{K^* 0 K^0 \gamma}) I_R, \quad (\text{A14})$$

where $R = G, F$ or H and I_R are the structure integrals given by

$$\begin{aligned} I_G &= \int_0^\infty \int_0^\infty \int_0^\infty \frac{d\alpha_1 d\alpha_2 d\alpha_3}{\Delta_1^3} \exp(B_3) L_1, \\ I_F &= \int_0^\infty \int_0^\infty \int_0^\infty \frac{d\alpha_1 d\alpha_2 d\alpha_3}{\Delta_1^2} \exp(B_3) L_2, \\ I_H &= \int_0^\infty \int_0^\infty \int_0^\infty \frac{d\alpha_1 d\alpha_2 d\alpha_3}{\Delta_1^2} \exp(B_3) L_3, \end{aligned} \quad (\text{A15})$$

$$B_3 = -\alpha_1 \mu_K^2 - \alpha_2 \mu_{K^*}^2 - \alpha_3 \mu_{B^*}^2 - \mu_{B_{s1}}^2 w_{B^* K} w_{KB^*} + \frac{\alpha_{3KB^*}}{\Delta_1} (\mu_{B_{s1}}^2 \alpha_{1B^* K} + \mu_{B_s^*}^2 \alpha_2), \quad (\text{A16})$$

and

$$\begin{aligned} L_1 &= -\frac{1}{\mu_{B^*}^2 (\mu_{B_{s1}}^2 - \mu_{B_s^*}^2)} \left((1 - \beta_{12})(\mu_{B_{s1}}^2 \beta_1 + \mu_{B_s^*}^2 (\beta_1 + \beta_2)) + 3(\mu_{B_{s1}}^2 - \mu_{B_s^*}^2) + \frac{3}{\Delta_1} \right), \\ L_2 &= -\left(2 + \frac{1}{\mu_{B^*}^2 \Delta_1} \right) (1 - \beta_1) + \beta_2 \left(3 + \frac{5}{\mu_{B^*}^2 \Delta_1} \right) - \beta_1 \beta_2 \left(1 - \frac{\mu_{B_{s1}}^2 + \mu_{B_s^*}^2}{\mu_{B^*}^2} + \frac{4}{\mu_{B^*}^2 \Delta_1} \right) \\ &\quad - \beta_2^2 \left(1 - 2 \frac{\mu_{B_s^*}^2}{\mu_{B^*}^2} + \frac{4}{\mu_{B^*}^2 \Delta_1} \right) - \beta_2^3 (3 - 4\beta_2) \frac{\mu_{B_s^*}^2}{\mu_{B^*}^2} - 2\beta_1 \beta_2^2 (1 - \beta_2) \frac{\mu_{B_{s1}}^2 + 2\mu_{B_s^*}^2}{\mu_{B^*}^2} \\ &\quad - \beta_1^2 \beta_2 (1 - \beta_2) \frac{2\mu_{B_{s1}}^2 + \mu_{B_s^*}^2}{\mu_{B^*}^2} + \beta_1^3 \beta_2 \frac{\mu_{2B_{s1}}^2}{\mu_{B^*}^2}, \\ L_3 &= -\beta_1 (1 - \beta_{12}), \quad \beta_1 = \frac{\alpha_{1B^* K}}{\Delta_1}, \quad \beta_2 = \frac{\alpha_2}{\Delta_1}, \quad \beta_{12} = \beta_1 + \beta_2. \end{aligned} \quad (\text{A17})$$

6. Decay $B_{s1}^* \rightarrow B_{s0}^* \gamma$.

The contribution to the coupling constant $G_{B_{s1}B_{s0}^*\gamma}$, coming from the diagrams in Figs.7(a,b) is defined by

$$G_{B_{s1}B_{s0}^*\gamma} = \frac{1}{16\pi^2 \Lambda^2} g_{B_{s1}} g_{B_{s0}^*} (g_{B^* \pm B^\pm \gamma} + g_{B^* 0 B^0 \gamma}) I_{B_{s1}B_{s0}^*\gamma}, \quad (\text{A18})$$

where $I_{B_{s1}B_{s0}^*\gamma}$ is the structure integral given by

$$\begin{aligned} I_{B_{s1}B_{s0}^*\gamma} &= \int_0^\infty \int_0^\infty \int_0^\infty \frac{d\alpha_1 d\alpha_2 d\alpha_3}{\Delta^3} \exp(B_4) (\alpha_3 + w_{B^* K} + w_{BK}), \\ B_4 &= -\alpha_1 \mu_{B^*}^2 - \alpha_2 \mu_B^2 - \alpha_3 \mu_K^2 - \mu_{B_{s1}}^2 w_{B^* K} w_{KB^*} - \mu_{B_{s0}^*}^2 w_{BK} w_{KB} \\ &\quad + \frac{\alpha_3 + w_{B^* K} + w_{BK}}{\Delta} (\mu_{B_{s1}}^2 \alpha_{1KB^*} + \mu_{B_{s0}^*}^2 \alpha_{2KB}), \\ \Delta &= 2 + \alpha_{123}. \end{aligned} \quad (\text{A19})$$

[1] J. L. Rosner, Phys. Rev. D **74**, 076006 (2006) [arXiv:hep-ph/0608102].
[2] T. Barnes, F. E. Close and H. J. Lipkin, Phys. Rev. D **68**, 054006 (2003) [arXiv:hep-ph/0305025].
[3] A. Faessler, T. Gutsche, V. E. Lyubovitskij and Y. L. Ma, Phys. Rev. D **76**, 014005 (2007) [arXiv:0705.0254 [hep-ph]].
[4] A. Faessler, T. Gutsche, S. Kovalenko and V. E. Lyubovitskij, Phys. Rev. D **76**, 014003 (2007) [arXiv:0705.0892 [hep-ph]].
[5] A. Faessler, T. Gutsche, V. E. Lyubovitskij and Y. L. Ma, Phys. Rev. D **76**, 114008 (2007) [arXiv:0709.3946 [hep-ph]].
[6] T. Branz, T. Gutsche and V. E. Lyubovitskij, arXiv:0712.0354 [hep-ph].
[7] Y. B. Dong, A. Faessler, T. Gutsche and V. E. Lyubovitskij, in preparation.
[8] S. Weinberg, Phys. Rev. **130**, 776 (1963); A. Salam, Nuovo Cim. **25**, 224 (1962); K. Hayashi, M. Hirayama, T. Muta, N. Seto and T. Shirafuji, Fortsch. Phys. **15**, 625 (1967).
[9] G. V. Efimov and M. A. Ivanov, *The Quark Confinement Model of Hadrons*, (IOP Publishing, Bristol & Philadelphia, 1993).
[10] I. V. Anikin, M. A. Ivanov, N. B. Kulimanova and V. E. Lyubovitskij, Z. Phys. C **65**, 681 (1995); M. A. Ivanov, M. P. Locher and V. E. Lyubovitskij, Few Body Syst. **21**, 131 (1996); M. A. Ivanov, V. E. Lyubovitskij, J. G. Körner and P. Kroll, Phys. Rev. D **56**, 348 (1997) [arXiv:hep-ph/9612463]; M. A. Ivanov, J. G. Körner, V. E. Lyubovitskij and A. G. Rusetsky, Phys. Rev. D **60**, 094002 (1999) [arXiv:hep-ph/9904421]; A. Faessler, T. Gutsche, M. A. Ivanov, V. E. Lyubovitskij and P. Wang, Phys. Rev. D **68**, 014011 (2003) [arXiv:hep-ph/0304031]; A. Faessler, T. Gutsche, M. A. Ivanov, J. G. Körner, V. E. Lyubovitskij, D. Nicmorus and K. Pumsa-ard, Phys. Rev. D **73**, 094013 (2006) [arXiv:hep-ph/0602193]; A. Faessler, T. Gutsche, B. R. Holstein, V. E. Lyubovitskij, D. Nicmorus and K. Pumsa-ard, Phys. Rev. D **74**, 074010 (2006) [arXiv:hep-ph/0608015].
[11] V. Baru, J. Haidenbauer, C. Hanhart, Yu. Kalashnikova and A. E. Kudryavtsev, Phys. Lett. B **586** (2004) 53 [arXiv:hep-ph/0308129]; C. Hanhart, Yu. S. Kalashnikova, A. E. Kudryavtsev and A. V. Nefediev, Phys. Rev. D **75**, 074015 (2007) [arXiv:hep-ph/0701214].
[12] S. Godfrey and R. Kokoski, Phys. Rev. D **43**, 1679 (1991).
[13] E. J. Eichten, C. T. Hill and C. Quigg, Phys. Rev. Lett. **71**, 4116 (1993) [arXiv:hep-ph/9308337].
[14] A. F. Falk and T. Mehen, Phys. Rev. D **53**, 231 (1996) [arXiv:hep-ph/9507311].
[15] D. Ebert, V. O. Galkin and R. N. Faustov, Phys. Rev. D **57**, 5663 (1998) [Erratum-ibid. D **59**, 019902 (1998)] [arXiv:hep-ph/9712318].
[16] W. A. Bardeen, E. J. Eichten and C. T. Hill, Phys. Rev. D **68** (2003) 054024 [arXiv:hep-ph/0305049].
[17] T. Matsuki, K. Mawatari, T. Morii and K. Sudoh, Phys. Lett. B **606** (2005) 329 [arXiv:hep-ph/0411034]; T. Matsuki and T. Morii, Phys. Rev. D **56**, 5646 (1997) [Austral. J. Phys. **50**, 163 (1997)] [arXiv:hep-ph/9702366].
[18] E. E. Kolomeitsev and M. F. M. Lutz, Phys. Lett. B **582**, 39 (2004) [arXiv:hep-ph/0307133].
[19] T. Matsuki, T. Morii and K. Sudoh, AIP Conf. Proc. **814**, 533 (2006) [arXiv:hep-ph/0510269].
[20] F. K. Guo, P. N. Shen, H. C. Chiang and R. G. Ping, Phys. Lett. B **641** (2006) 278 [arXiv:hep-ph/0603072].
[21] F. K. Guo, P. N. Shen and H. C. Chiang, Phys. Lett. B **647** (2007) 133 [arXiv:hep-ph/0610008].
[22] P. Colangelo, F. De Fazio and R. Ferrandes, Nucl. Phys. Proc. Suppl. **163**, 177 (2007) [arXiv:hep-ph/0609072].
[23] J. Vijande, A. Valcarce and F. Fernandez, arXiv:0711.2359 [hep-ph].
[24] Z. G. Wang, arXiv:0712.0118 [hep-ph].
[25] F. K. Guo, S. Krewald and U. G. Meissner, arXiv:0712.2953 [hep-ph].
[26] Z. G. Wang, arXiv:0801.0267 [hep-ph].
[27] Z. G. Wang, arXiv:0801.1932 [hep-ph].
[28] Z. G. Wang, arXiv:0803.1223 [hep-ph].
[29] J. Gasser and H. Leutwyler, Nucl. Phys. B **250**, 465 (1985).
[30] P. L. Cho and M. B. Wise, Phys. Rev. D **49**, 6228 (1994) [arXiv:hep-ph/9401301].
[31] P. Colangelo and F. De Fazio, Phys. Lett. B **570**, 180 (2003) [arXiv:hep-ph/0305140].
[32] T. Mehen and R. P. Springer, Phys. Rev. D **70**, 074014 (2004) [arXiv:hep-ph/0407181].
[33] W. M. Yao *et al.* [Particle Data Group], J. Phys. G **33** (2006) 1.
[34] S. Mandelstam, Annals Phys. **19**, 1 (1962); J. Terning, Phys. Rev. D **44**, 887 (1991).
[35] Y. Dong, A. Faessler, T. Gutsche and V. E. Lyubovitskij, Phys. Rev. D **77**, 094013 (2008) [arXiv:0802.3610 [hep-ph]].
[36] A. Anastassov *et al.* [CLEO Collaboration], Phys. Rev. D **65**, 032003 (2002) [arXiv:hep-ex/0108043].
[37] Z. G. Wang and S. L. Wan, Phys. Rev. D **74**, 014017 (2006) [arXiv:hep-ph/0606002].
[38] M. E. Bracco, A. J. Cerqueira, M. Chiapparini, A. Lozea and M. Nielsen, Phys. Lett. B **641**, 286 (2006) [arXiv:hep-ph/0604167].
[39] F. S. Navarra, M. Nielsen and M. E. Bracco, Phys. Rev. D **65**, 037502 (2002) [arXiv:hep-ph/0109188].
[40] Z. W. Lin and C. M. Ko, Phys. Rev. C **62**, 034903 (2000) [arXiv:nucl-th/9912046].
[41] M. B. Wise, Phys. Rev. D **45**, R2188 (1992).
[42] R. Casalbuoni, A. Deandrea, N. Di Bartolomeo, R. Gatto, F. Feruglio and G. Nardulli, Phys. Rept. **281**, 145 (1997) [arXiv:hep-ph/9605342].
[43] J. A. M. Vermaasen, arXiv:math-ph/0010025.

TABLE I: Decay widths of $B_{s0}^* \rightarrow B_s\pi$ and $B_{s1} \rightarrow B_s^*\pi^0$ in keV. The range of values for our results is due to the variation of Λ_M from 1 to 2 GeV.

| Approach | $\Gamma(B_{s0}^* \rightarrow B_s\pi^0)$ | Approach | $\Gamma(B_{s1} \rightarrow B_s^*\pi^0)$ |
|-------------|---|-------------|---|
| Ref. [16] | 21.5 | Ref. [16] | 21.5 |
| Ref. [20] | 1.54 | Ref. [21] | 10.36 |
| Ref. [27] | 6.8 – 30.7 | Ref. [27] | 5.3 – 20.7 |
| Our results | 55.2 – 89.9 | Our results | 57.0 – 94.0 |

TABLE II: Decay widths of $B_{s0}^* \rightarrow B_s^*\gamma$ and $B_{s1} \rightarrow B_s\gamma$ in keV. The range of values for our results is due to the variation of Λ_M from 1 to 2 GeV.

| Approach | $\Gamma(B_{s0}^* \rightarrow B_s^*\gamma)$ | Approach | $\Gamma(B_{s1} \rightarrow B_s\gamma)$ |
|-------------|--|-------------|--|
| Ref. [16] | 58.3 | Ref. [16] | 39.1 |
| Ref. [23] | 171.4 | Ref. [23] | 106.5 |
| Ref. [23] | 31.9 | Ref. [23] | 60.7 |
| Ref. [28] | 1.3 – 13.6 | Ref. [28] | 3.2 – 15.8 |
| Our results | 3.07 – 4.06 | Our results | 2.01 – 2.67 |

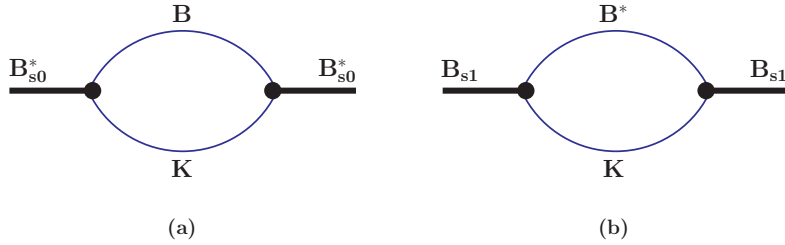


FIG. 1: Mass operators of B_{s0}^* and B_{s1} mesons.

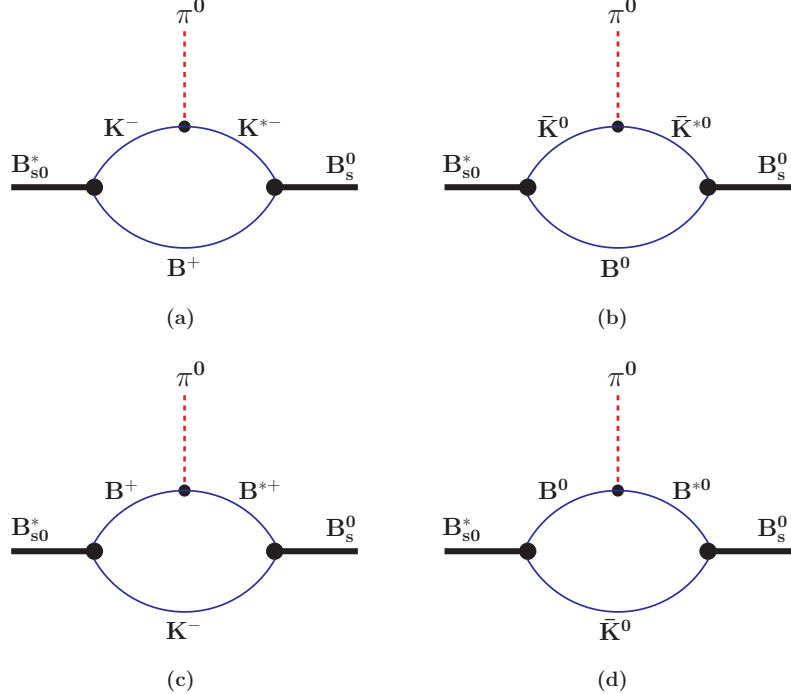


FIG. 2: Diagrams contributing to the strong transition $B_{s0}^* \rightarrow B_s + \pi^0$.

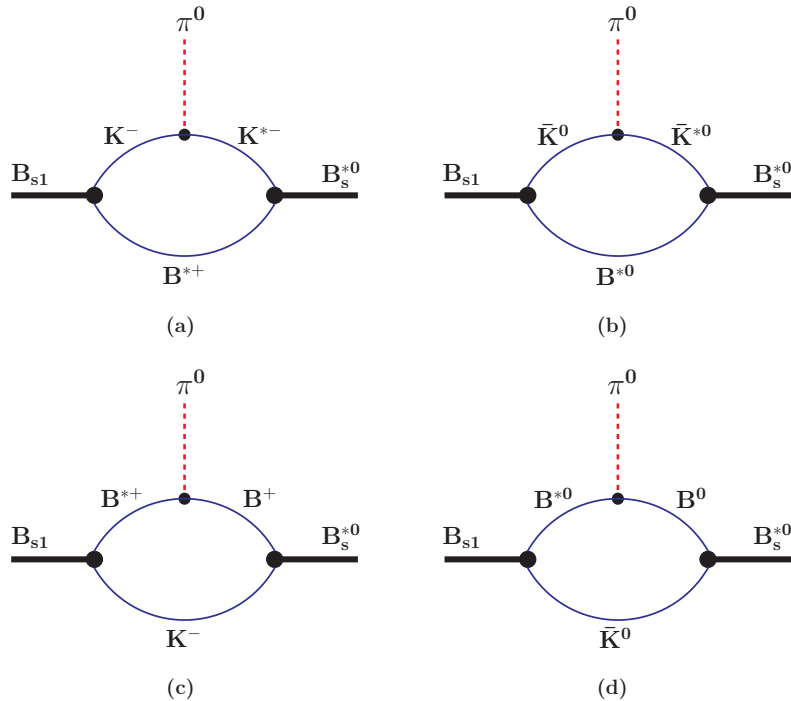
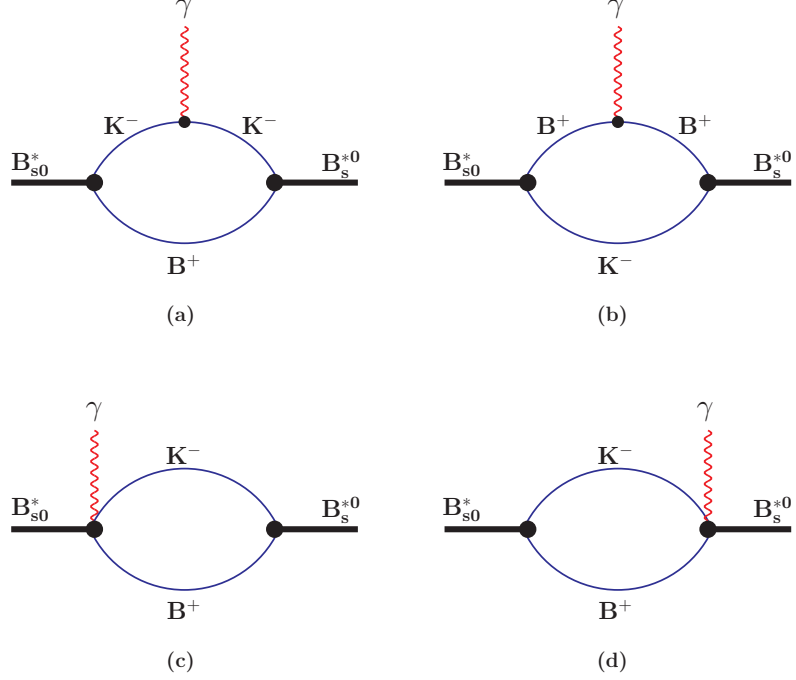
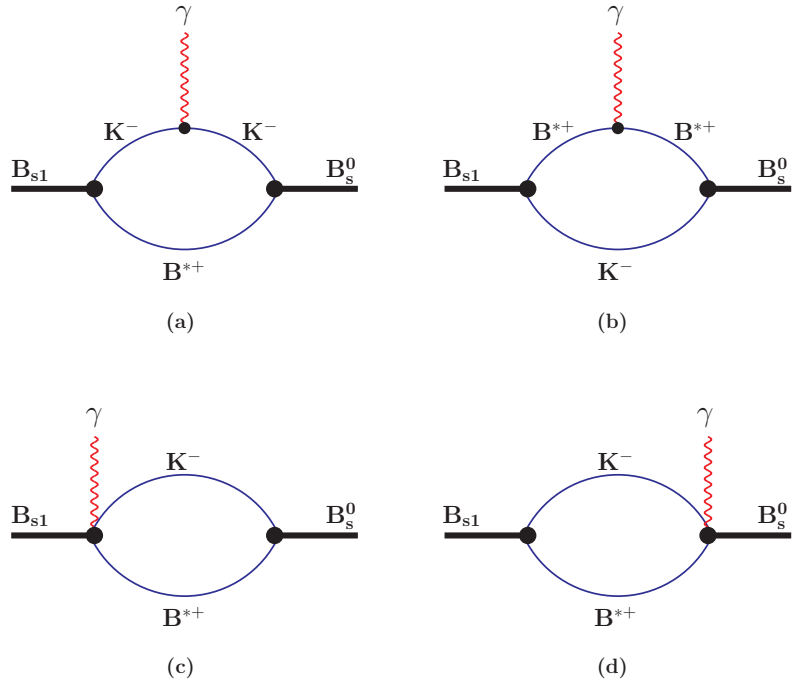


FIG. 3: Diagrams contributing to the strong transition $B_{s1} \rightarrow B_s^* + \pi^0$.

FIG. 4: Diagrams contributing to the radiative transition $B_{s0}^* \rightarrow B_s^* + \gamma$.FIG. 5: Diagrams contributing to the radiative transition $B_{s1} \rightarrow B_s + \gamma$.

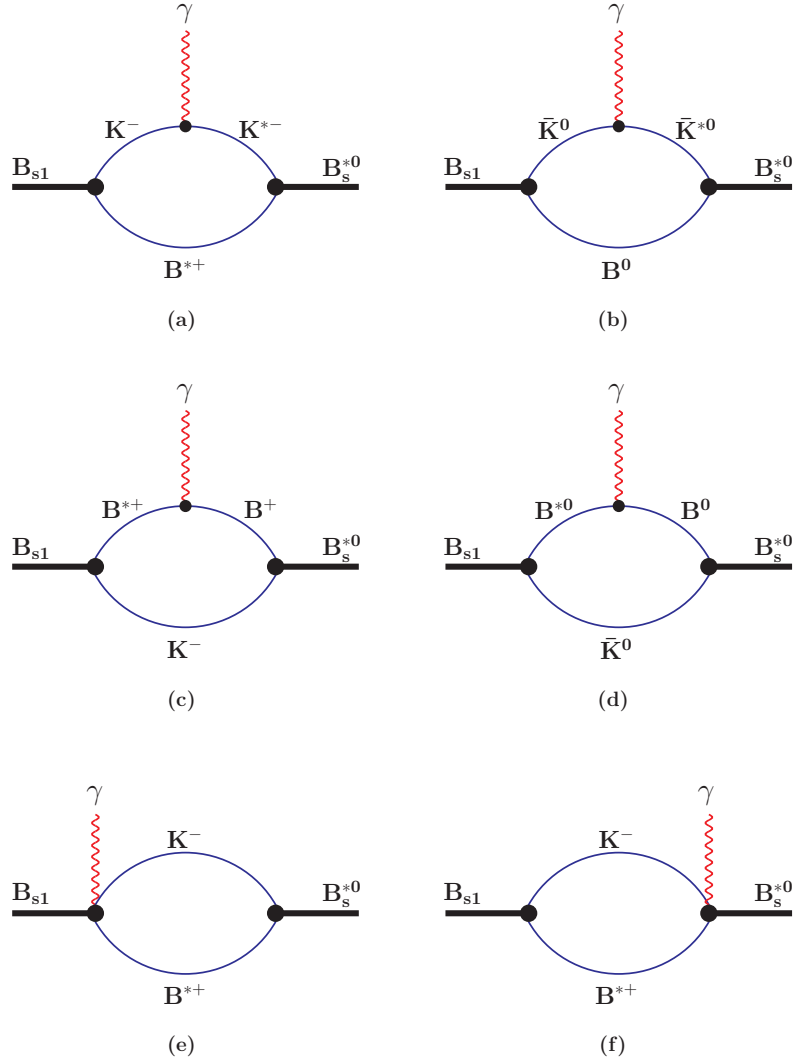


FIG. 6: Diagrams contributing to the radiative transition $B_{s1} \rightarrow B_s^* + \gamma$.

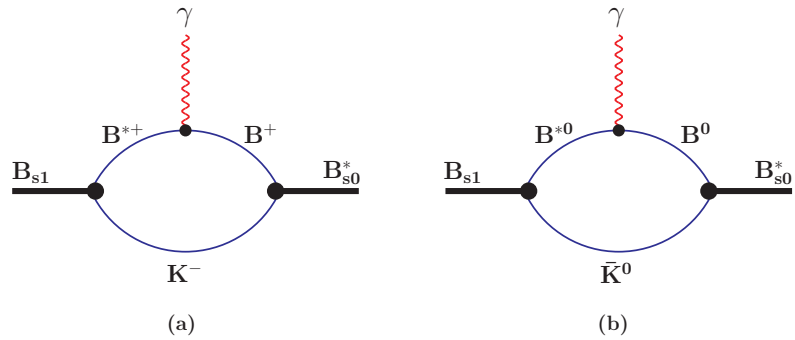


FIG. 7: Diagrams contributing to the radiative transition $B_{s1} \rightarrow B_{s0}^* + \gamma$.